This article has been accepted for publication in a future issue of this journal, but has not been fully edited. Content may change prior to final publication. Citation information: DOI 10.1109/TMC.2014.2307332, IEEE Transactions on Mobile Computing

Joint Mobile Data Gathering and Energy Provisioning in Wireless Rechargeable Sensor Networks

Songtao Guo[1], Cong Wang[2], and Yuanyuan Yang[2]

[1]*School of Electronic and Information Engineering, Southwest University, Chongqing, 400715, P.R. China*
[2]*Department of Electrical & Computer Engineering, Stony Brook University, Stony Brook NY 11794, USA*

***Abstract*—The emerging wireless energy transfer technology enables charging sensor batteries in a wireless sensor network (WSN) and maintaining perpetual operation of the network. Recent breakthrough in this area has opened up a new dimension to the design of sensor network protocols. In the meanwhile, mobile data gathering has been considered as an efficient alternative to data relaying in WSNs. However, time variation of recharging rates in wireless rechargeable sensor networks imposes a great challenge in obtaining an optimal data gathering strategy. In this paper, we propose a framework of joint Wireless Energy Replenishment and anchor-point based Mobile Data Gathering (WerMDG) in WSNs by considering various sources of energy consumption and time-varying nature of energy replenishment. To that end, we first determine the anchor point selection strategy. and the sequence to visit the anchor points. We then formulate the WerMDG problem into a network utility maximization problem which is constrained by flow, energy balance, link and battery capacity and the bounded sojourn time of the mobile collector. Furthermore, we present a distributed algorithm composed of cross-layer data control, scheduling and routing subalgorithms for each sensor node, and sojourn time allocation subalgorithm for the mobile collector at different anchor points. We also provide the convergence analysis of these subalgorithms. Finally, we implement the WerMDG algorithm in a distributed manner in the NS-2 simulator and give extensive numerical results to verify the convergence of the proposed algorithm and the impact of utility weight, link capacity and recharging rate on network performance.**

***Index Terms*—Mobile data gathering, energy replenishment, distributed algorithms, rechargeable sensor networks.**

I. Introduction

Currently, wireless sensor networks (WSNs) are mainly powered by batteries. Due to limited energy storage capacity of a sensor battery, WSNs can usually remain operational only for a limited amount of time. However, in many applications, such as earthquake, soil monitoring and glacial movement monitoring, due to the harshness of the environment, a long period of unattended operability is required. Although there has been a flourish of research efforts on prolonging the lifetime of WSNs, network lifetime remains a performance bottleneck of WSNs and one of the key factors that hinder their large scale deployment.

On the other hand, it has been shown that energy harvesting from natural sources, such as solar, wind, thermal and vibration can effectively improve network performance and prolong network lifetime. However, the success of extracting energy from the environment remains limited in practice. This is because that the outcome of energy-harvesting highly depends on the environment. For example, in a solar harvesting system, the amount of harvested energy is determined by the time and strength of solar radiation.

Besides harvesting environmental energy to prolong network lifetime, how to gather sensed data is one of the most important tasks in WSNs. In [1], [3], optimal data collection rates for sensor nodes to forward data to a static data sink was studied in energy harvesting networks. These schemes belong to relay-routing based static data gathering, and may lead to non-uniform energy consumption among all the sensors and more congestion and packet loss at the sensors closer to the static sink. To overcome these problems, mobile data gathering has been proposed recently, see, for example, [2], [4], [6], [9], [10], [12], in which one or more mobile collectors are employed to collect data from sensors. Since the routing task has been partially or fully taken over by the mobile collector, this approach can effectively eliminate the non-uniformity of energy consumption among sensor nodes and alleviate the heavy traffic load of sensor nodes closer to the data sink.

In the meanwhile, recent breakthrough in wireless energy transfer technology due to Kurs, et al. [13] has opened up a new dimension to prolonging sensor network lifetime. It was shown in [13] that by exploiting coupled magnetic resonance, it is feasible to transfer energy wirelessly between two coils. Their experiment showed that with this technology it is capable of transferring 60 watts with about 40% efficiency over a distance of 2 meters. Intel has also demonstrated [14] that wireless recharging is effective for transferring 60 watts of power over a distance of up to two to three meters with efficiency of 75%. On the other hand, recent advances in Radio Frequency (RF)-based wireless energy transfer can also increase sustainability of WSNs [15]–[17]. Clearly, wireless energy transfer will have a profound impact on the design of WSNs, which is attributed to its following advantages: (1) it can provide reliable energy without being affected by the dynamics of environments; (2) it eliminates wires or plugs between the charger and receiver; (3) it does not interfere with the normal operations of sensors such as sensing, packets delivering and receiving.

Inspired by the novel energy transfer technology and motivated by the benefit of mobile data gathering, Zhao, et al. [8] proposed a joint design of energy replenishment and mobile data gathering (J-MERDG) by establishing a flow-level network utility maximization model to characterize the data gathering performance. Although this scheme can effectively collect data and save energy by utilizing mobile collectors, it considers energy consumption only in data transmission but not in data receiving and sensing, and regards recharging rates as constant instead of time-varying. However, in practice, the time varying profile of recharging rates poses challenges in computing optimal data rates.

Based on these observations, in this paper, we present a comprehensive scheme of joint wireless energy replenishment and mobile data gathering (WerMDG), which considers all types of sensor energy consumptions and the time-varying nature of recharging time. The proposed scheme has the following advantages. First, since the mobile collector directly provides electric energy to sensors by wireless energy transfer, energy delivery will no longer suffer from environmental variations such as weather or seasonal effects. Second, as long as the mobile collector stays close to sensors, a steady and high recharging rate can be achieved to ensure the high-rate data service. Third, the mobility of the mobile collector can alleviate the routing burden of sensors so that energy can be saved to further prolong network lifetime.

In particular, the objective of this paper is to provide a distributed and adaptive solution that jointly selects the sensors to be recharged, finds the optimal data generating and uploading rates and the optimal scheduling and routing paths for each node, and determines the optimal sojourn time for the mobile collector at each anchor point, such that the overall network utility can be maximized. To that end, we first formulate the WerMDG problem as an optimization problem. Then we convert the original non-convex WerMDG problem into a convex one by employing some auxiliary variables, and separate the convex optimization problem into two levels of optimization by taking a hierarchical decomposition approach.

The main contributions of the paper can be summarized below. First, we consider comprehensive sources of energy consumption including transmission, reception and sensing, and the time-varying nature of energy recharging, to better characterize real networks. Second, we propose a WerMDG optimization framework under flow conservation, energy balance, link and battery capacity, and the bounded sojourn time. Third, we develop a proximal approximation based cross-layer algorithm to obtain the system-wide optimum by adjusting data rates, link scheduling and flow routing for each sensor, and allocating sojourn time for the mobile collector in a distributed manner. Finally, we validate the convergence and effectiveness of the proposed algorithm by extensive numerical results and evaluate the impact of utility weight, link capacity and recharging rate on network performance.

The remainder of this paper is organized as follows. Section II discusses related work. Section III introduces the network model and anchor point selection process. Section IV outlines the proposed framework and transforms the non-convex WerMDG problem into a convex problem. Section V presents the distributed algorithms. Section VI provides numerical results. Finally, Section VII concludes the paper.

II. Related Works

A. Energy Harvesting Networks and Data Collection

Prolonging sensor lifetime in energy harvesting/rechargeable networks has recently attracted considerable attention in the wireless networking research community. In [1], [3], the authors proposed solutions for fair and high throughput data extraction in the presence of renewable energy sources, which aims to compute the lexicographically maximum data collection rate for each node. Chen, et al. [5] considered the problem of maximizing throughput over a finite-horizon time period for a sensor network with energy replenishment. Liu, et al. [7] studied the problem of joint energy management and resource allocation in rechargeable sensor networks to maximize network utility while maintaining perpetual operation. In addition, energy harvesting techniques have been considered along with the traditional data collection with a static data sink.

In the meanwhile, utility maximization problem for mobile data gathering in WSN has been considered in [6], [8], [9], [11], [12]. In [6], [8], Zhao, et al. formalized the mobile data gathering problems as network utility maximization problems under the constraints of guaranteed network lifetime and data gathering latency. In [9], data collection performance was further improved by equipping the vehicle with multiple antennas to allow concurrent uploading. The network utility maximization was studied in [11] for MANETs with lossy links such that the rate-outage probability is within some arbitrarily small target tolerance. In [12], a transmission scheduling algorithm was studied for wireless sensor networks with high node densities, where a mobile sink is responsible for gathering the data packets from the sensor nodes with similar observations. However, these works do not consider the current battery energy of sensor node in energy balance constraint and the energy consumptions in receiving and sensing data. In this paper, we account for the node's battery energy in energy constraint and energy consumptions comprised of transmission/reception/sensing.

B. Wireless Energy Transfer

Recently, there have been great research efforts in the area of wireless energy transfer. It was shown that wireless energy residing in the radio frequencies can be effectively captured to power small devices such as sensors in [15]–[17]. In order to achieve timely and efficient charging, Erol-Kantarci and Mouftah [15] proposed a sustainable wireless rechargeable sensor network (SuReSense) which employs mobile chargers that charge multiple sensors from several landmark locations. In [16], Chiu, et al. studied mobility-aware charger deployment for wireless rechargeable sensor networks with an objective of maximizing the survival rate of end-devices. In [17], He, et al. considered reader (energy provider) deployment, point provisioning and path provisioning in a wireless rechargeable sensor network to ensure the WISP tags (energy receivers) can harvest sufficient energy for continuous operation. In addition to wireless energy transfer via radio frequencies, energy transfer through magnetic coupling can usually support higher amount of energy transfer in short time with high efficiency. Its application in WSNs was envisioned in [18] and [8]. Shi, et al. [18] considered the scenario of a mobile charging vehicle periodically traveling inside a sensor network with static data collection and recharging each sensor node's battery wirelessly. Zhao, et al. [8] combined wireless energy transfer with mobile data collection and formulated the problem into a utility maximization problem. However, mobile data collection was not considered in [18], while the energy consumptions in receiving data and the time-varying nature of recharging process were not reflected in the analysis in [8]. Moreover, the works overlook the fact that the recharge process brings the energy gradually to the level of battery capacity. In [19], wireless charging and mobile data collection in WSNs were jointly studied and distributed algorithms on how to select data rates, adjust link flow and recharge sojourn time were proposed. However, only results on individual nodes were provided. In this paper, we further improve the algorithms in [19] by exploring various features of the network and evaluating the algorithms in a network-wide environment, to deliver a more comprehensive and in-depth solution to fully capture the practical aspects missing in [8], [18], [19].

C. Efficient Resource Allocation

There have been some previous works on distributed and adaptive selection of sensors to be recharged and efficient routing in mobile sensor/ad hoc/opportunistic networks [3], [6]–[8], [20]–[22]. In [3], [6], [7], the authors designed solutions that jointly compute data collection rates for each node, find routes and schedule transmissions. Similar to our work, Zhao, et al. [8] gave a solution in which the locations of a subset of sensors are periodically selected as anchor points and proposed a distributed algorithm to adjust data rates, link scheduling and flow routing. However, these works do not consider the current battery energy of sensor node and the time-varying nature of recharging process

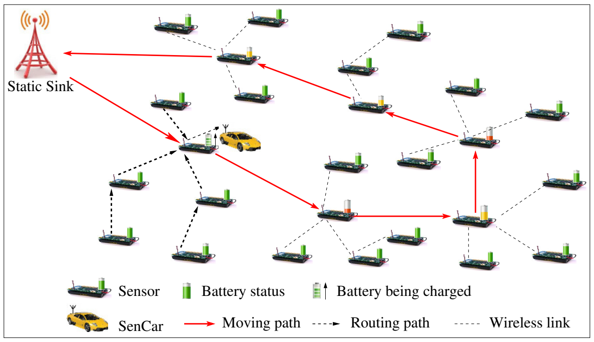

Fig. 1. Joint wireless energy replenishment and mobile data gathering.

in their distributed algorithm. Zhang, et al, proposed a harvesting aware utility-based sensing rate allocation algorithm [20] whereas they focused on the environmental energy harvesting instead of wireless charging, and did not deal with the problem of how to select sensor nodes to be recharged.

In [21], a joint opportunistic power scheduling and end-to-end rate control scheme was presented for wireless ad hoc networks by modeling the time-varying wireless channel as a stochastic process. In [22], the authors modeled an efficient spatial-TDMA based adaptive power and rate cross-layer scheduling problem as a mixed integer linear program . However, these works do not adopt mobile data gathering and do not consider the impact from wireless energy replenishment on link scheduling and data routing, whereas we combine these two aspects in our formulations.

III. Network Model and Anchor Point Selection

A. Network Model

We consider a network consisting of stationary rechargeable sensor nodes and a static sink. In the sensing field, as shown in Fig. 1, we deploy a multi-functional mobile collector, called *SenCar*, which could be a mobile robot or vehicle equipped with a powerful transceiver to gather data. The SenCar is also equipped with a resonant coil as energy transmitter as well as a high capacity battery to store sufficient energy. The SenCar periodically visits some pre-defined sensor positions called *anchor points* in the field and stays at each anchor point for a period of *sojourn time*.

Let B_i denote the battery capacity of node i and $\mathcal{N}$ be the set of all the nodes in the network. All sensors in the coverage area of anchor point a form a neighboring set of the anchor point, denoted by $\mathcal{N}^a$. The neighboring set is determined in a way that nodes can communicate with the sensor node at the anchor point in l hops. The choice of l will have an impact on energy consumption of sensor nodes, i.e., a larger l can cover more sensor nodes from an anchor point location with higher energy consumption on intermediate nodes, whereas a smaller l can save energy on intermediate nodes but cover fewer sensor nodes. In practice, l is chosen such that the anchor points can cover all the sensor nodes in the network. The SenCar starts from the static sink (starting position) and roams over the entire sensing field in a pre-determined sequence of anchor points, at a certain traveling speed V_s (in m/s). The SenCar gathers data directly from sensors by visiting the anchor points in a periodic data gathering tour. When the SenCar moves to an anchor point a, it will stay at the anchor point for a period of sojourn time τ^a to replenish battery energy of the node at the anchor point and gather the data uploaded by sensors in l hops. After τ^a time, the SenCar leaves anchor point a and travels to the next anchor point.

For data gathering, we consider a simple interference model in this paper, the *node-exclusive interference model*, in which any two links are not allowed to share a common node to transmit at the same time. Otherwise, a collision occurs and the transmission is discarded. We assume the network is sparse so that the impact of channel access and packet collision on the optimal solution is minimum.

We also assume the energy replenished into sensor's battery is much larger than the energy consumed due to transmission, sensing activities and the amount of energy consumed at the anchor points would be compensated by wireless recharge. Thus, when the SenCar finishes recharging and leaves an anchor point, the node at the anchor point is recharged to a high energy level. Since nodes closer to the anchor points consume more energy, these nodes are more likely to be the candidates of anchor points in the next interval.

To compute the energy replenished during sojourn time τ^a, let $\rho_i^a(t)$ denote the instantaneous energy replenishment rate of node i at anchor point a in time t, and π_i^a represent the average replenishment energy for sensor i during a period of sojourn time τ^a which is defined as $\pi_i^a = \int_0^{\tau^a} \rho_i^a(t)dt$. It is worth pointing out that in contrast to [8], we take into consideration of the recharging time for a sensor battery; on the other hand, we assume that the SenCar spends short time to replace its own battery at the data sink and compute the sequence of anchor points to visit in its next trip.

B. Anchor Point Selection

Choosing anchor points is a crucial step of the data gathering process since it determines the efficiency of energy transferring and the latency of data gathering. A trivial scheme is to simply visit all the sensor nodes, gather data through single-hop transmission and use the SenCar to forward data back to the static sink through long range communications. However, this scheme would trigger several new problems in our data collection and wireless recharge scheme.

First, using single-hop data collection can only collect data from a very small number of nodes per interval. Only the nodes reside at the anchor points are able to transmit data while data generated at other nodes is not collected. Therefore, the fairness of data collection among all the nodes is greatly undermined in single hop data collection. In contrast, if multi-hop transmission is used, we can collect data from the larger neighborhood of anchor points thereby improving the fairness of data collection. Second, the average packet latency will be increased with single-hop communication. Since if nodes are not visited by the SenCar, their data packets would be buffered until these nodes are selected as anchor points. It would result in longer average data collection latency and is not scalable for large networks. In contrast, in our proposed solution, the SenCar only visits a subset of selected sensor nodes (anchor points) and collects data through multi-hop transmissions, which can enhance data collection fairness, reduce data collection latency, and avoid stopping at unnecessary sensor locations for battery recharge.

On the other hand, although directly forwarding data back to the static sink via long range communication seems to be more efficient, such a scheme involves high energy cost. Let e_t be the energy consumption of transmitting packets of length l_p, d_r be the distance between the SenCar and the static sink, and α be the path loss exponent (usually 2-4). Since $e_t \propto d_r^\alpha l_p$ [23], the energy cost would be prohibitively high when the sensing field is large (e.g., $500 \times 500m^2$). Thus, directly forwarding data via long range communication is not scalable in large networks consisting of hundreds of thousands of nodes or with high rate data services. In the proposed model, our objective is to achieve a reasonable balance between data gathering latency and energy replenishment.

In wireless rechargeable sensor networks, as each sensor has different energy status at different time, it is desirable to recharge as many sensors with low energy as possible to ensure the perpetual operation of sensors. Accordingly, the sensors located at the selected anchor points should be those with the most urgent needs of energy supplement. In the meanwhile, to better enjoy the benefit of the energy supply provided by the SenCar, more anchor points should be selected. However, this would prolong the traveling tour length and increase the data gathering latency. Thus, it is an inherent tradeoff between the number of sensors to be recharged in a tour and the data gathering latency. Based on these observations, when determining the sequence of anchor points to visit, we jointly consider the remaining energy levels of sensors and the traveling tour length of the SenCar. Our anchor point selection algorithm can be described as follows.

When the SenCar completes data gathering for the sensors in its neighbor set $\mathcal{N}^a$ at anchor point a during a tour, each sensor i in $\mathcal{N}^a$ will report its current battery status or remaining battery energy b_i to the SenCar. The SenCar then will utilize this information to determine the sequence to visit anchor points at the beginning of the next tour.

After the SenCar receives the current battery energy status $\{b_i\}$ of all the sensors, it sorts the sensors in an increasing order according to their battery energy $\{b_i\}$, and records the sorted sensor list by $\mathcal{S}'$, where $\mathcal{S}'(i)$ denotes the i-th element in list $\mathcal{S}'$. Thus $\mathcal{S}'$ is a sorted list of all sensor nodes containing battery information in the network. The SenCar searches for the maximum number of anchor points for the next tour in the sorted sensor list such that the tour length is no more than a threshold L_{tsp}, i.e., finds a target sensor (candidate anchor point) $\mathcal{S}'(n)$ such that by visiting the sensors with an index no more than n, i.e., $\mathcal{S}'(1), \mathcal{S}'(2), ..., \mathcal{S}'(n)$, the tour length of the SenCar is no more than a bound L_{tsp}.

To find target sensor $\mathcal{S}'(n)$, the algorithm first searches the middle element of $\mathcal{S}'$, denoted by $\mathcal{S}'(m)$, and then inspects the shortest traveling tour among the locations of sensors $\mathcal{S}'(1), \mathcal{S}'(2), ..., \mathcal{S}'(m)$. Note that in order to facilitate the computing of the tour length of the SenCar, the locations of sensors are regarded as the candidate anchor points. The traveling tour can be found by a binary search algorithm and an approximate solution to Traveling Salesman Problem (TSP). Here, we use the TSP Nearest Neighbor algorithm [24] to find the shortest traveling tour of the SenCar. If the traveling tour length equals the bound L_{tsp}, then the target sensor is found; otherwise, the upper half or the lower half of the list is chosen to further search for the target sensor based on whether the tour length of the SenCar is more than or less than the bound L_{tsp}. The anchor point selection algorithm is given in Table I. In the algorithm, sorting sensor list by the divide and conquer method needs $\mathcal{O}(|\mathcal{N}| \log |\mathcal{N}|)$ time. In the worst case, searching the target sensor requires at most $\lceil \log |\mathcal{N}| \rceil$ rounds by binary search algorithm. In each round, we need to calculate the shortest tour among at most $|\mathcal{N}|$ sensors, and the approximate TSP algorithm needs $\mathcal{O}(|\mathcal{N}|^2)$ time to search for the shortest tour. The total time of the anchor points selection algorithm is $\mathcal{O}(|\mathcal{N}| \log |\mathcal{N}| + |\mathcal{N}|^2 \log |\mathcal{N}|)$. In the worst case, the time complexity of the selection algorithm is $\mathcal{O}(|\mathcal{N}|^2 \log |\mathcal{N}|)$.

TABLE I
ANCHOR POINT SELECTION ALGORITHM

```
**Inputs**: Sensor list $\mathcal{N}$, battery status $\{b_i\}$, and tour bound $L_{tsp}$;
**Outputs**: Anchor point list $\mathcal{A}$;
Sort sensor list $\mathcal{N}$ in an ascending order according to battery status $\{b_i\}$
and record the result in $\mathcal{S}'$; $u$ = 1, $v = |\mathcal{S}'|$, $n = 0$, $m = 0$;
while $true$ do
  if $u > v$ then $n = v$; break; end if
  $m = \lfloor \frac{1}{2}(u + v) \rfloor, \mathcal{A} = \{\mathcal{S}'(1), \mathcal{S}'(2), \cdots, \mathcal{S}'(m)\}$;
  Calculate the shortest tour length by TSP Nearest
  Neighbor Algorithm (TSP-NN) for anchor points in $\mathcal{A}$ and
  let TSP-NN($\mathcal{A}$) denote its tour length;
  case
    TSP-NN($\mathcal{A}$) $< L_{tsp}$: $u = m + 1$;
    TSP-NN($\mathcal{A}$) $= L_{tsp}$: $n = m$; break;
    TSP-NN($\mathcal{A}$) $> L_{tsp}$: $u = m - 1$;
  end case
end while
$\mathcal{A} = \{\mathcal{S}'(1), \mathcal{S}'(2), \cdots, \mathcal{S}'(n)\}$
```

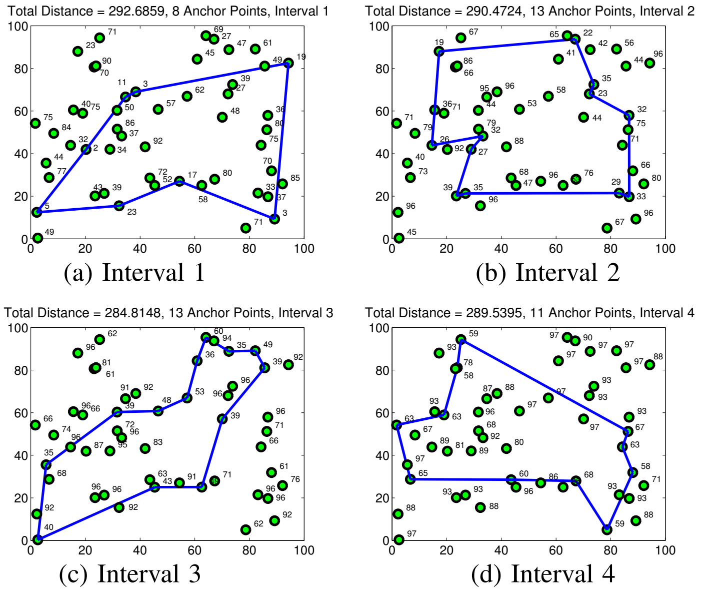

(a) Interval 1 (b) Interval 2 (c) Interval 3 (d) Interval 4

Fig. 2. Evolution of anchor point selections in 4 consecutive intervals when $L_{tsp} = 300m$.

An example of evolution of anchor points in four consecutive intervals is illustrated in Fig. 2, where 50 sensor nodes with initial battery energy uniformly distributed over [0,100]% are randomly deployed on a 100 × 100 m^2 field. We set the data collection hop count $l = 3$ and and utilize the Nearest Neighbor heuristic algorithm [24] to find the shortest TSP route. By setting $L_{tsp} = 300m$, we can see the selection of anchor points is evolving according to the current energy level in each interval. Since data is collected in multi-hop at anchor points, nodes closer to anchor points consume more energy than other nodes, thus they are more likely to become anchor points in the next interval.

After the anchor points and the sequence to visit them are determined, the remaining issue is how to gather data from sensors when the SenCar migrates among the anchor points, which we will discuss next.

IV. Problem Formulation

In this section, we formulate the WerMDG problem into a utility maximization problem under flow conservation, energy balance and link capacity.

We model the sensor network with the SenCar located at anchor point a as a directed graph $G^a = (V^a, E^a)$. $V^a = \mathcal{N} \cup \{s^a\}$ consists of all sensor nodes and the SenCar at the anchor point, denoted by s^a. $E^a = \{(i,j) | i,j \in V^a\}$ represents the set of directed links among the sensors and the SenCar. A directed link $(i,j) \in E^a$ exists if $d_{ij} \leq R_{tx}$, where d_{ij} denotes the distance

TABLE II
LIST OF NOTATIONS

Notation	Definition
$\mathcal{N}$	Set of sensor nodes
s^a	SenCar located at anchor point a
$\mathcal{A}$	Set of anchor points
$\mathcal{N}^a$	Set of neighbor sensor nodes of anchor point a
τ^a	Sojourn time of SenCar at anchor point a
π_i^a	Average replenishment energy for sensor i during τ^a
$\mathcal{S}'$	Sorted sensor list
E^a	Set of directed links among sensors and SenCar at anchor point a
L_{tsp}	Bound of traveling tour length for SenCar
r_i^a	Data rate of sensor i when SenCar is at anchor point a
$f_{ij}^{(a)}$	Flow rate over link (i,j) when SenCar is located at anchor point a
C_{ij}^a	Capacity of link (i,j) when SenCar is at anchor point a
B_i	Battery capacity of sensor i
b_i	Current battery energy status of sensor i
$\rho_i^a(t)$	Instantaneous energy recharging rate of sensor i at anchor point a in time t
μ_{ij}^{tx}	Energy consumption for delivering a packet over link (i,j)
μ_i^{rx}	Energy consumption for receiving a packet at sensor i
μ_i^{gn}	Energy consumption for generating a packet at sensor i
ζ_i	Minimum remaining energy of sensor i
V_s	Moving velocity of SenCar
T	Bound of total sojourn time

between node i and node j, and R_{tx} stands for the transmission range of sensor nodes. f_{ij}^a represents the flow rate over link (i,j) at anchor point a. Sensor $i \in \mathcal{N}$ generates data for the SenCar at a data rate of r_i^a when the SenCar moves to anchor point a. For each sensor node $i \in \mathcal{N}$, we assume that it consumes different energy in different working stages. To elaborate, μ_{ij}^{tx} denotes the energy consumption of sensor i delivering a packet over link (i,j), μ_i^{rx} represents the energy consumption for receiving a packet at node i, and μ_i^{gn} denotes the energy consumption for generating a packet in the sensing environment at node i. These notations and their corresponding definitions are summarized in Table II.

In our model, in order to characterize the effect of the data from a sensor on the overall data gathering performance, we assume that each sensor i attains a utility function $U_i(\cdot)$, which is twice-differentiable, increasing and strictly concave with respect to the total amount of data gathered from sensor i in a data gathering tour (i.e.,$\sum_{a\in\mathcal{A}} r_i^a\tau^a$). Our objective is to maximize the network utility under flow conservation, energy balance and link capacity while maintaining the perpetual operation of the network. With the given sequence to visit anchor points, we can formulate the joint wireless energy replenishment and mobile data gathering (WerMDG) problem in rechargeable sensor networks into the following optimization problem:

$$\textbf{OPT-1}: \quad \max_{\mathbf{r},\,\mathbf{f},\,\tau} \sum_i U_i(\sum_{a\in\mathcal{A}} r_i^a\tau^a) \tag{1}$$

subject to

$$r_i^a + \sum_{j:(j,i)\in E^a} f_{ji}^a = \sum_{j:(i,j)\in E^a} f_{ij}^a, \forall i\in\mathcal{N}, \forall a\in\mathcal{A} \tag{2}$$

$$\tau^a \left(\sum_{j:(i,j)\in E^a} f_{ij}^a\mu_{ij}^{tx} + \sum_{j:(j,i)\in E^a} f_{ji}^a\mu_i^{rx} + r_i^a\mu_i^{gn} \right)$$

$$\leq b_i + \int_0^{\tau^a} \rho_i^a(t)dt - \zeta_i, \forall i\in\mathcal{N}, \forall a\in\mathcal{A} \tag{3}$$

$$0 \leq f_{ij}^a \leq C_{ij}^a, \forall (i,j)\in E^a, \forall a\in\mathcal{A} \tag{4}$$

$$b_i + \int_0^{\tau^a} \rho_i^a(t)dt \leq B_i, \forall i\in\mathcal{N}, \forall a\in\mathcal{A} \tag{5}$$

$$\sum_{a\in\mathcal{A}} \tau^a \leq T \tag{6}$$

where $\mathbf{r} = \{r_i^a | i\in\mathcal{N}, a\in\mathcal{A}\}$, $\mathbf{f} = \{f_{ij}^a | (i,j)\in E^a, a\in\mathcal{A}\}$, $\tau = \{\tau^a | a\in\mathcal{A}\}$ and ζ_i is an arbitrarily small positive constant, which represents the minimum remaining energy of sensor i to avoid being drained.

Constraints (2)-(6) can be explained as follows. Flow conservation constraint (2) states that the aggregated outgoing link flow rates at each sensor equal the incoming link flow rates plus its local data rate. Energy balance constraint (3) enforces that the average energy consumption for transmission, reception and sensing should be slightly less than the sum of the current battery energy b_i of sensor node i and the average charged energy income during a period of sojourn time τ^a. This constraint ensures that sensor nodes would not deplete their battery energy.

Link capacity constraint (4) specifies that the flow rate allocated on link (i,j) should be within the capacity of that link. Battery capacity constraint (5) demonstrates that the sum of the current battery energy b_i of sensor node i and the recharging energy for its battery cell cannot exceed its battery capacity, which is justified by the fact that the recharge process brings the energy gradually to the level of battery capacity while the recharging rate is decreasing. In our paper, this process is mathematically modeled by $\rho_i^a(t) = \alpha B(i)e^{-\alpha t}$ (applicable to most energy storage devices such as capacitor, energy cells and batteries), so the amount of energy replenished in τ^a time is $\int_0^{\tau^a} \alpha B(i)e^{-\alpha t}dt = B(i) - B(i)e^{-\alpha\tau^a}$ which approaches $B(i)$ when $\tau^a \to \infty$. Thus, when the SenCar stays at the anchor point for indefinitely long time, it can recharge the node battery to 100% but cannot surpass the battery capacity. Finally, sojourn time constraint (6) shows that the total data gathering latency is bounded by T.

It is worth noting that energy balance constraint (3) takes into account of the energy consumptions due to transmission and reception for multi-hop routing. To elaborate, for an intermediate node i in multi-hop routing, since it needs to forward all the data received towards anchor point a through its neighboring nodes, it consumes energy $\sum_{j:(i,j)\in E^a} f_{ij}^a\mu_{ij}^{tx}$ by summing up all the traffic forwarded to its neighboring nodes j. On the other hand, it consumes $\sum_{j:(j,i)\in E^a} f_{ji}^a\mu_i^{rx}$ energy to receive packets from all its neighboring nodes. For example, if we need to transmit packets from node 1 to anchor point a through node 3, then the energy consumption on intermediate nodes is $f_{13}^a\mu_{13}^{tx} + r_3^a\mu_3^{gn} + f_{3a}^a\mu_{3a}^{tx}$.

The objective of optimization problem (**OPT-1**) is to find the optimal data rate for each sensor and the proper flow rate for each link, and determine the optimal routing of the data from sensors to the SenCar and the optimal sojourn time of the SenCar for gathering data, when the SenCar moves over different anchor points such that the network utility can be maximized.

In general, problem (**OPT-1**) is non-convex since the objective function $U_i(\cdot)$ is not strictly concave with respect to r_i^a and τ^a due to the coupling between the optimization variables r_i^a and τ^a and the linearity of $\sum_{a\in\mathcal{A}} r_i^a\tau^a$, even though it is strictly concave with respect to the total data amount $\sum_{a\in\mathcal{A}} r_i^a\tau^a$ from sensor i.

To break down the couplings and make problem (**OPT-1**) solvable, we need to introduce auxiliary variables x_{ij}^a, y_i and ϕ_i^a and convert problem (**OPT-1**) into an equivalent convex problem. Let $x_{ij}^a = f_{ij}^a\tau^a$, $y_i\phi_i^a = r_i^a\tau^a$, $\phi_i^a \geq 0$, and $\sum_a \phi_i^a = 1$, where x_{ij}^a denotes the flow amount over link (i,j) destined to the SenCar at anchor point a during τ^a, y_i represents the total amount of data generated by sensor i in a data gathering tour, and ϕ_i^a is a data split variable, such that $\phi_i^a \geq 0$, and $\sum_a \phi_i^a = 1$, which determines the portion of the data uploaded by sensor i to the SenCar at anchor point a over the total amount of data generated by sensor i in a

This article has been accepted for publication in a future issue of this journal, but has not been fully edited. Content may change prior to final publication. Citation information: DOI 10.1109/TMC.2014.2307332, IEEE Transactions on Mobile Computing

data gathering tour. One of the reasons why a sensor node splits its data to be uploaded is that when the SenCar stays at an anchor point, a sensor may upload all or part of data, which depends on the allocated optimal sojourn time at this anchor point. Short sojourn time may cause some sensors not to have enough time to upload all the data. Thus these sensors have to upload the remaining data to other anchor points.

By multiplying the link capacity constraint and flow conservation by τ^a and using these auxiliary variables, we can reformulate optimization problem (**OPT-1**) into a convex optimization problem (**OPT-2)** with respect to $\mathbf{x}$, $\mathbf{y}$, τ and ϕ as follows.

$$\textbf{OPT-2}: \quad \max_{\mathbf{x},\,\mathbf{y},\,\tau,\,\phi} \sum_{i\in\mathcal{N}} U_i(y_i) \tag{7}$$

subject to

$$y_i\phi_i^a + \sum_{j:(j,i)\in E^a} x_{ji}^a = \sum_{j:(i,j)\in E^a} x_{ij}^a, \forall i\in\mathcal{N}, \forall a\in\mathcal{A} \tag{8}$$

$$\sum_{j:(i,j)\in E^a} x_{ij}^a\mu_{ij}^{tx} + \sum_{j:(j,i)\in E^a} x_{ji}^a\mu_i^{rx} + y_i\phi_i^a\mu_i^{gn} \le b_i + \int_0^{\tau^a}\rho_i^a(t)dt - \zeta_i, \forall i\in\mathcal{N}, \forall a\in\mathcal{A} \tag{9}$$

$$0\le x_{ij}^a \le C_{ij}^a\tau^a, \forall (i,j)\in E^a, \forall a\in\mathcal{A} \tag{10}$$

$$b_i + \int_0^{\tau^a}\rho_i^a(t)dt \le B_i, \forall i\in\mathcal{N}, \forall a\in\mathcal{A} \tag{11}$$

where $\mathbf{x} = \{x_{ij}^a|(i,j)\in E^a, a\in\mathcal{A}\}$, $\mathbf{y} = \{y_i|i\in\mathcal{N}\}$, $\phi = \{\phi_i^a|i\in\mathcal{N}, a\in\mathcal{A}\}$, $\sum_a\tau^a\le T$ and $\sum_a\phi_i^a = 1$.

Since the objective function $\sum_{i\in\mathcal{N}}U_i(y_i)$ is concave with respect y_i while the constraint set composed by (8)-(11) is convex, optimization problem (**OPT-2)** is a strictly convex optimization problem, however, with nonlinear constraints (8) and (9), which are induced by the coupling between y_i and ϕ_i^a. To decompose the coupling variables y_i and ϕ_i^a in constraints (8) and (9), we employ a hierarchical decomposition approach [6] [26] to separating optimization problem (**OPT-2)** into a repeated two-level optimization problem, which first maximizes the network utility over $\mathbf{x}$, $\mathbf{y}$ and τ while keeping ϕ fixed, then maximizes the network utility by updating ϕ. Next, we will discuss the two-level optimization problem in detail.

V. Distributed Algorithm for WerMDG Problem

In this section, we employ a hierarchical decomposition approach to separating optimization problem (**OPT-2)** into two levels of optimization to decompose coupling variables y_i and ϕ_i^a. At the lower level, we provide a distributed algorithm for data control, routing and sojourn time allocation by solving the following optimization problem, denoted as **OPT-2a**, that maximizes network utility over variables $\mathbf{x}$, $\mathbf{y}$ and τ while keeping ϕ fixed.

$$\textbf{OPT-2a}: \quad \max_{\mathbf{x},\,\mathbf{y},\,\tau} \sum_{i\in\mathcal{N}} U_i(y_i) \tag{12}$$

subject to constraints (8)-(11) and $\sum_a\tau^a\le T$.

At the higher level, our goal is to determine the optimal proportion of uploading data to the SenCar at different anchor points by considering the following data split problem, denoted as **OPT-2b**, that maximizes network utility by updating ϕ.

$$\textbf{OPT-2b}: \quad \max_{\phi} U(\phi) \tag{13}$$

subject to

$$\sum_a \phi_i^a = 1, \forall i\in\mathcal{N} \tag{14}$$

$$\phi_i^a \ge 0, \forall i\in\mathcal{N}, \forall a\in\mathcal{A} \tag{15}$$

where $U(\phi)$ is the optimal objective value of problem (**OPT-2a)** over $\mathbf{x}$, $\mathbf{y}$ and τ.

A. Lower Level Optimization

Since optimization problem (**OPT-2a**) is strictly convex, in this subsection, we use Lagrangian dual decomposition [26] approach to solve it. We first relax constraints (8), (9) and (10) by introducing Lagrangian multipliers λ_i^a, ν_i^a and ξ_{ij}^a, respectively. Then we can obtain the partial Lagrangian of optimization problem (**OPT-2a**).

$$\begin{aligned} L(\mathbf{x},\mathbf{y},\tau,\lambda,\nu,\xi) &= \sum_{i\in\mathcal{N}} U_i(y_i) - \sum_{i\in\mathcal{N}}\sum_{a\in\mathcal{A}}\left(\lambda_i^a\phi_i^a + \nu_i^a\phi_i^a\mu_i^{gn}\right)y_i \\ &+ \sum_{a\in\mathcal{A}}\sum_{j:(i,j)\in E^a}\left(\lambda_i^a - \lambda_j^a - \nu_i^a\mu_{ij}^{tx} - \nu_j^a\mu_j^{rx} - \xi_{ij}^a\right)x_{ij}^a \\ &+ \sum_{i\in\mathcal{N}}\sum_{a\in\mathcal{A}}\nu_i^a\left(b_i + \int_0^{\tau^a}\rho_i^a(t)dt - \zeta_i\right) + \sum_{a\in\mathcal{A}}\sum_{(i,j)\in E^a}\xi_{ij}^a C_{ij}^a\tau^a \end{aligned}$$

Here, λ_i^a can be interpreted as the flow conservation price at sensor i for the SenCar at anchor point a, ν_i^a can be regarded as the energy balance price to ensure the perpetual operation of each sensor node, and ξ_{ij}^a can be referred to as the link capacity price over link (i,j) at anchor point a.

We define the objective function of the Lagrangian dual problem as

$$D(\lambda,\nu,\xi) = \max_{\mathbf{x},\mathbf{y},\tau} L(\mathbf{x},\mathbf{y},\tau,\lambda,\nu,\xi) \tag{16}$$

with constraint (11). By duality, the dual problem of the primal problem is given by

$$\min_{\lambda,\nu,\xi\succeq 0} D(\lambda,\nu,\xi) \tag{17}$$

We can observe that the maximization problem in the dual function has been decomposed into three independent subproblems: data control at the transport layer, joint scheduling and routing (flow control) at the network layer, and sojourn time allocation for the SenCar at different anchor points, which implies that the WerMDG problem can be separated and solved in a distributed manner. The first two subproblems are separately solved by each sensor while the last one is implemented in the SenCar. It can be seen that the decomposition corresponds to a vertical decomposition across the protocol stack. The subproblems of data control and joint scheduling and routing are coordinated by flow conservation price λ and energy balance price ν. Moreover, energy balance price ν should be sent from each sensor to the SenCar for solving the sojourn time allocation subproblem. In the following, we give the corresponding distributed subalgorithms of data control, routing and sojourn time allocation.

1) ***Data control subalgorithm****:* The data control subalgorithm aims to determine the optimal amount of data generated by sensor i in a data gathering tour by solving the following local optimization problem.

$$\max_{\mathbf{y}\succeq\mathbf{0}} U_i(y_i) - \sum_{a\in\mathcal{A}}\left(\lambda_i^a\phi_i^a + \nu_i^a\phi_i^a\mu_i^{gn}\right)y_i \tag{18}$$

subject to constraint (20).

Since $y_i = \sum_a y_i\phi_i^a \le \sum_a\sum_j x_{ij}^a$, which is due to the fact that the generated data amount from sensor i in a data gathering tour is no more than the total flow amount forwarded by sensor i to the SenCar, we have

$$\sum_a\sum_j x_{ij}^a \le \sum_a\sum_j C_{ij}^a\tau^a \le T\sum_a\sum_j C_{ij}^a. \tag{19}$$

This indicates that variable y_i has an upper bound $Q_i = T\sum_a\sum_j C_{ij}^a$, i.e.,

$$0\le y_i\le Q_i. \tag{20}$$

TABLE III
DISTRIBUTED DATA CONTROL SUBALGORITHM FOR SENSOR i

```
Compute $Q_i = T\sum_a \sum_j C^a_{ij}$, for all $j : (i, j) \in E^a$ and $a \in \mathcal{A}$;
for all $a \in \mathcal{A}$
   Obtain the Lagrangian multipliers $\lambda^a_i$ and $\nu^a_i$;
   Compute $\varpi_i = \sum_{a\in\mathcal{A}}(\lambda^a_i \phi^a_i + \nu^a_i \phi^a_i \mu^{gn}_i)$;
   if $\varpi_i < U'_i(Q_i)$ then $y_i = Q_i$;
   else if $\varpi_i > U'_i(0)$ then $y_i = 0$;
   else $y_i \ = U'^{-1}_i(\varpi_i)$
   end if
end for
```

Since data control subproblem (18) is concave with respect to y_i, the Karush-Kuhn-Tucker (KKT) conditions are satisfied and there is no duality gap. Thus, the primal and dual problems have optimal solutions. We introduce Lagrangian multiplier α_i for constraint $y_i \leq Q_i$, and β_i for constraint $y_i \geq 0$. Let y^*_i be the optimal solution to problem (18). For all $i \in \mathcal{N}$, the KKT conditions can be given by

$$\begin{aligned} & U'_i(y^*_i) - \sum_{a\in\mathcal{A}}(\lambda^{a*}_i \phi^a_i + \nu^{a*}_i \phi^a_i \mu^{gn}_i) - \alpha^*_i + \beta^*_i = 0 \\ & \alpha^*_i(y^*_i - Q_i) = 0 \\ & \beta^*_i y^*_i = 0, \alpha^*_i \geq 0, \beta^*_i \geq 0 \end{aligned} \tag{21}$$

where $U'_i(y^*_i)$ denotes the first-order derivative of U_i with respect to y_i. For clarity, we use $g(y_i)$ to denote the objective function in (18). For $0 \leq y^*_i \leq Q_i$, we have the following three cases according to the KKT conditions in (21).

1) If $\alpha^*_i > 0$, then $y^*_i = Q_i$, $\beta^*_i = 0$, and $\alpha^*_i = U'_i(y^*_i) - \sum_{a\in\mathcal{A}}(\lambda^{a*}_i \phi^a_i + \nu^{a*}_i \phi^a_i \mu^{gn}_i) = \frac{\partial g(y^*_i)}{\partial y_i} > 0$;
2) If $\alpha^*_i = 0$ and $\beta^*_i = 0$, then $y^*_i \in [0, Q_i]$, and $U'_i(y^*_i) - \sum_{a\in\mathcal{A}}(\lambda^{a*}_i \phi^a_i + \nu^{a*}_i \phi^a_i \mu^{gn}_i) = \frac{\partial g(y^*_i)}{\partial y_i} = 0$;
3) If $\beta^*_i > 0$, then $y^*_i = 0$, $\alpha^*_i = 0$ and $-\beta^*_i = U'_i(y^*_i) - \sum_{a\in\mathcal{A}}(\lambda^{a*}_i \phi^a_i + \nu^{a*}_i \phi^a_i \mu^{gn}_i) = \frac{\partial g(y^*_i)}{\partial y_i} < 0$.

From the above cases, we find that the exact value or the range of y_i corresponds to the different values of $\frac{\partial g(y_i)}{\partial y_i}$. As U_i is a strictly concave function, U'_i decreases with the increase of y_i. Since $0 \leq y_i \leq Q_i$, it is clear that $U'_i(Q_i) \leq U'_i(y_i) \leq U'_i(0)$. For brevity, we use ϖ_i to denote $\sum_{a\in\mathcal{A}}(\lambda^a_i \phi^a_i + \nu^a_i \phi^a_i \mu^{gn}_i)$. Given Lagrangian multipliers λ and ν for the current subgradient iteration, we should first calculate the value of ϖ_i, and then determine the value of y_i based on the relationship between ϖ_i , $U'_i(Q_i)$ and $U'_i(0)$. To elaborate, if $\varpi_i < U'_i(Q_i)$, which indicates case 1) is satisfied, then $y_i = Q_i$; if $\varpi_i > U'_i(0)$, which implies case 3) is satisfied, then $y_i = 0$; otherwise, the value of y_i is updated by $y_i = U'^{-1}_i(\varpi_i)$. This subalgorithm is summarized in Table III. It is apparent that to find the solution of y^*_i, sensor i needs to examine at most $|\mathcal{A}|$ anchor point. Thus the time complexity of the data control subalgorithm for sensor i is $O(|\mathcal{A}|)$. It is not difficult to observe that the subalgorithm can be implemented by each sensor in a distributed manner without any additional message passing, and its convergence depends on two aspects: one is the prices of flow conservation and energy balance; the other is the number of anchor points sensor i belongs to.

*2) **Joint scheduling and routing subalgorithm**:* The joint scheduling and routing subalgorithm aims to schedule link activation and determine routing of data from sensor i to the SenCar so as to allocate the optimal flow amount on scheduled links destined to anchor point a during τ^a. In practice, there could be some control messages generated in the process of scheduling and routing such as link gain message, matched/drop message, and the messages on energy balance prices and link capacity prices in sojourn time allocation subalgorithm, however, compared to data packets, these messages are of much smaller sizes and are transmitted less frequently. Thus, the control messages can be ignored at the flow level characterization of the problem. The objective can be achieved by solving the following maximization problem at sensor i.

$$\max_{\mathbf{x}\succeq\mathbf{0}} \sum_{a\in\mathcal{A}} \sum_{j:(i,j)\in E^a} \left(\lambda^a_i - \lambda^a_j - \nu^a_i \mu^{tx}_{ij} - \nu^a_j \mu^{rx}_j - \xi^a_{ij}\right) x^a_{ij} \tag{22}$$

subject to

$$\sum_{a\in\mathcal{A}} \sum_{j:(i,j)\in E^a} (\mu^{tx}_{ij} + \mu^{rx}_j) x^a_{ij} \leq B_i - \zeta_i \tag{23}$$

$$0 \leq \sum_{a\in\mathcal{A}} \sum_{j:(i,j)\in E^a} x^a_{ij} \leq \sum_{a\in\mathcal{A}} \sum_{j:(i,j)\in E^a} C^a_{ij} T \tag{24}$$

where constraint (23) is the combination of constraints (9) and (11), which specifies that the energy consumption for delivering and receiving at node i cannot exceed its maximum available energy budget, and constraint (24) is due to the fact that the total sojourn time at all the anchor points is bounded by T as indicated in (19), and $(\lambda^a_i - \lambda^a_j - \nu^a_i \mu^{tx}_{ij} - \nu^a_j \mu^{rx}_j - \xi^a_{ij})$ can be regarded as the gain of link (i, j) scheduled to transmit data. It is clear that for the optimal solution to (22), sensor i should spend all its energy budget $\mathcal{E}^b_i = B_i - \zeta_i$ on the traffic flows over the link with the largest positive gain.

Without loss of generality, we let $x^a_{ij,\max} = C^a_{ij} T$ and define $w^a_{ij} = \lambda^a_i - \lambda^a_j - \nu^a_i \mu^{tx}_{ij} - \nu^a_j \mu^{rx}_j - \xi^a_{ij}$. In fact, problem (22) is a joint scheduling and routing problem. We first consider the scheduling problem, i.e., for sensor i, find a preferred outgoing neighbor j^* and a designated anchor point a^* such that $(j^*, a^*)_i = \arg\max_{j,a} \left[w^a_{ij}\right]^+$ and allocate a flow amount $\widetilde{x}^{a^*}_{ij}$ for link (i, j) at anchor point a^* such that

$$\widetilde{x}^{a^*}_{ij} = \arg \max_{x^{a^*}_{ij} \in \left[0, x^{a^*}_{ij,\max}\right]} \sum_{j:(i,j)\in E^{a^*}} w^{a^*}_{ij} x^{a^*}_{ij} \tag{25}$$

The scheduling problem is equivalent to the maximum weighted matching problem, that is, to maximize the weighted sum of the link capacities with the schedulability constraint under the node exclusive interference model. We can utilize the sequential greedy algorithm similar to that in [27] to solve scheduling problem (25) distributively in linear time $O(|E^a|)$. The basic idea of the greedy algorithm for the scheduling problem is that sensor i finds node j^* such that $w^a_{ij^*}$ is maximized over all links $(i, j) \in E^a$ with unmatched neighbor j, and takes advantage of RTS/CTS handshaking to match node i and node j^*. To elaborate, if sensor i has received a *matching* request from j^*, then link (i, j^*) is a matched link and node i sends a *matched* reply to j^* and a *drop* message to all other unmatched neighbors; otherwise, node i sends a *matching* request to node j^*, and upon receiving a matched reply from j^*, node i knows that link (i, j^*) is a matched link and node i sends a *drop* message to all other unmatched neighbors.

Now we consider the routing problem. Sensor i sends an amount of bits over link (i, j^*) to the SenCar at anchor point a^*, i.e.,

$$x^a_{ij} = \begin{cases} \min\left\{\frac{\mathcal{E}^b_i}{\mu^{tx}_{ij} + \mu^{rx}_j}, x^a_{ij,\max}\right\}, \text{if } (j, a)_i = (j^*, a^*)_i \\ 0, \quad \text{otherwise} \end{cases} \tag{26}$$

It is clear that sensor i always allocates a maximum flow under the constraint of energy budget based on (26) to a scheduled link (i, j^*) that has the largest link gain among all its outgoing links to different anchor points. The joint scheduling and routing

TABLE IV
DISTRIBUTED JOINT SCHEDULING AND ROUTING SUBALGORITHM FOR SENSOR i

```
Set $x_{ij}^a = 0$, for all $j : (i,j) \in E^a, a \in \mathcal{A}$, initialize $B_i$ and $\zeta_i$;
Collect the price information from its neighbor $j$;
Compute $W_i = \{(j,a)|\lambda_i^a - \lambda_j^a - \nu_i^a \mu_{ij}^{tx} - \nu_j^a \mu_j^{rx} - \xi_{ij}^a > 0,$
    $\text{for all } j : (i,j) \in E^a, \forall a \in \mathcal{A}\}$; $\mathcal{E}_i^b = B_i - \zeta_i$;
while $W_i \neq \Phi$ for all $j : (i,j) \in E^a, \forall a \in \mathcal{A}$ do
  Calculate $w_{ij}^a = \lambda_i^a - \lambda_j^a - \nu_i^a \mu_{ij}^{tx} - \nu_j^a \mu_j^{rx} - \xi_{ij}^a$;
  Find $(j^*, a^*)_i = \arg\max_{(j,a)\in W_i} w_{ij}^a$ by scheduling algorithm;
  Calculate $w_{ij^*}^{a^*} = w_{ij}^a|_{(j,a)_i=(j^*,a^*)_i}$;
  Pass this information to its neighbors;
  Allocate $x_{ij}^a$ over link $(i, j^*)$ such that
    $x_{ij^*}^{a^*} = \min\left\{\frac{\mathcal{E}_i^b}{\mu_{ij^*}^{tx}+\mu_{j^*}^{rx}}, x_{ij^*,\max}^{a^*}\right\}$;
  Update $W_i$ by removing $(j^*, a^*)_i$ from it;
  $\mathcal{E}_i^b = \mathcal{E}_i^b - x_{ij^*}^{a^*}\left(\mu_{ij^*}^{tx} + \mu_{j^*}^{rx}\right)$;
end while
```

subalgorithm for sensor i is described in Table IV. Apparently, in the worst case, the time complexity of the subalgorithm for sensor i is $O(\sum_{a\in\mathcal{A}} |E^a|)$.

Notes that optimization problem (22) is linear and in turn is not strictly concave, which implies that the values in the optimal solution of the Lagrangian dual cannot be directly applied to primal problem (**OPT-2**). In view of this, we employ the primal recovery method introduced in [28]to recover the optimal values for variables x_{ij}^a. When variable ϕ_i^a converges in the higher level optimization, for the n-th subgradient iteration in the lower level optimization, we can calculate the adjusted primal feasible sequence $\left\{\widehat{x}_{ij}^a(k)\right\}$ as follows.

$$\widehat{x}_{ij}^a(k) = \frac{1}{k}\sum_{h=1}^{k} x(h) = \begin{cases} x_{ij}^a(1), & k = 1 \\ \frac{n-1}{n}\widehat{x}_{ij}^a(k-1) + \frac{1}{k}x_{ij}^a(k), & k > 1 \end{cases} \tag{27}$$

It was proved in [28] that when the diminishing stepsize is used, any accumulation point of sequence $\left\{\widehat{x}_{ij}^a(n)\right\}$ generated by (27) is feasible to the primal problem, and can converge to a primal optimal solution. Thus, optimal flow amount of each outgoing link for sensor i can be obtained when $\left\{\widehat{x}_{ij}^a(n)\right\}$ converges to $\widehat{x}_{ij}^{a*}$.

*3) **Sojourn time allocation subalgorithm**:* We now give a sojourn time allocation subalgorithm, the objective of which is to allocate the proper sojourn time for each anchor point by solving the following optimization problem.

$$\max_{\tau} \sum_{a\in\mathcal{A}}\sum_{i\in\mathcal{N}} \nu_i^a \left(b_i + \int_0^{\tau^a} \rho_i^a(t)dt - \zeta_i\right) + \sum_{a\in\mathcal{A}}\sum_{(i,j)\in E^a} \xi_{ij}^a C_{ij}^a \tau^a \tag{28}$$

subject to

$$b_i + \int_0^{\tau^a} \rho_i^a(t)dt \leq B_i, \forall i \in \mathcal{N}, \forall a \in \mathcal{A} \tag{29}$$

$$0 \leq \sum_{a\in\mathcal{A}} \tau^a \leq T \tag{30}$$

TABLE V
SOJOURN TIME ALLOCATION SUBALGORITHM FOR ANCHOR POINT a

```
Initialize $\sigma^a$;
repeat
  Receive $\nu_i^a$ for all sensor $i \in \mathcal{N}$ and $\xi_{ij}^a$ for all $(i,j) \in E^a$
     at anchor point $a$
  Compute the subgrandients $\nabla g(\tau^a)(k)$ and $\nabla g(\sigma^a)(k)$ by (33)
    and (34), respectively;
  Compute $\tau^a(k)$ by (31);
  Updates Lagrangian multiplier $\sigma^a(k+1)$ by (32);
until $\{\sigma^a(k)\}$ converges to $\sigma^{a*}$.
```

We know that the sojourn time allocation problem (28) is convex, and thus we can employ a subgradient projection with a sufficiently small step-size to solve the problem. Introducing Lagrangian multiplier σ^a for constraint (29), which can be referred to as the shadow price of sojourn time allocation at anchor point a, for all $a \in \mathcal{A}$, the sojourn time variable τ^a and the Lagrangian multiplier σ^a can be updated by

$$\tau^a(k+1) = \min\left\{[\tau^a(k) - \varepsilon(k)\nabla g(\tau^a)(k)]^+, T - \sum_{b\in\mathcal{A}\backslash a} \tau^b\right\} \tag{31}$$

$$\sigma^a(k+1) = [\sigma^a(k) + \varepsilon(k)\nabla g(\sigma^a)(k)]^+ \tag{32}$$

where

$$\nabla g(\tau^a)(k) = \sum_{i\in\mathcal{N}} (\nu_i^a - \sigma^a)\rho_i^a(\tau^a(k)) + \sum_{(i,j)\in E^a} \xi_{ij}^a C_{ij}^a \tag{33}$$

and

$$\nabla g(\sigma^a)(k) = -\sum_{i\in\mathcal{N}} \left(b_i + \int_0^{\tau^a(k)} \rho_i^a(t)dt - B_i\right) \tag{34}$$

denote the subgradients with respect to τ^a and σ^a, respectively; $[x]^+ = \max(0, x)$ and $\varepsilon(k)$ is a properly chosen step size. It is worth mentioning that the above updates are for the case that the SenCar at anchor point a recharges multiple sensors simultaneously. The sojourn time allocation subalgorithm for anchor point a is listed in Table V. Clearly, for the SenCar to determine sojourn time τ^a at anchor point a, the values of energy balance prices ν_i^a and link capacity prices ξ_{ij}^a need to be sent to the SenCar in each subgradient iteration. For the optimum solution τ^{a*} to the sojourn time allocation subproblem, we have $\nabla g(\tau^{a*})(k) = 0$, i.e.,

$$\sigma^{a*} = \nu_i^{a*} - \sum_{j:(i,j)\in E^a} \xi_{ij}^{a*} C_{ij}^a / \rho_i^a(\tau^{a*}(k)), \tag{35}$$

which indicates that the shadow price of sojourn time allocation is determined by not only the recharged energy of sensor nodes, but also the price of energy balance keeping sensor nodes available perpetually and the price of link capacity specifying the flow rate over a link no more than its maximum achievable flow rate.

From the above analysis, we can see that sojourn time vector $\tau^* \succeq 0$ is the optimal solution to optimization problem (28) if and only if there exists a shadow price vector $\sigma^* \succeq 0$ such that for each anchor point $a \in \mathcal{A}$ and sensor $i \in \mathcal{N}$, $\sigma^{a*}[\sum_{i\in\mathcal{N}}(\int_0^{\tau^{a*}} \rho_i^a(t)dt - B_i)] = 0$ and equation (35) is satisfied. As a result, to find the optimal solution, we gradually vary prices ν_i^a and ξ_{ij}^a, derive shadow price σ^a and further obtain sojourn time τ^a. When shadow price σ^a iteratively converges to its optimum σ^{a*}, the optimal solution to the sojourn time allocation problem is achieved.

*4) **Lagrangian multiplier update**:* In each iteration of the subalgorithms of data control, routing and sojourn time allocation, sensor i solves the subproblems in (18), (22) and (28) with the current Lagrangian multipliers $\lambda_i^a(k)$, $\nu_i^a(k)$ and $\xi_{ij}^a(k)$, where k denotes the index of subgradient iterations. Sensor i updates its Lagrangian multipliers according to

$$\lambda_i^a(k+1) = [\lambda_i^a(k) + \varepsilon(k)\nabla L(\lambda_i^a)(k)]^+ \tag{36}$$

$$\nu_i^a(k+1) = [\nu_i^a(k) + \varepsilon(k)\nabla L(\nu_i^a)(k)]^+ \tag{37}$$

$$\xi_{ij}^a(k+1) = \left[\xi_{ij}^a(k) + \varepsilon(k)\left(x_{ij}^a(k) - C_{ij}^a\tau^a(k)\right)\right]^+ \tag{38}$$

This article has been accepted for publication in a future issue of this journal, but has not been fully edited. Content may change prior to final publication. Citation information: DOI 10.1109/TMC.2014.2307332, IEEE Transactions on Mobile Computing

where

$$\nabla L(\lambda_i^a)(k) = y_i(k)\phi_i^a - \left(\sum_{j:(i,j)\in E^a} x_{ij}^a(k) - \sum_{j:(j,i)\in E^a} x_{ji}^a(k) \right)$$

$$\nabla L(\nu_i^a)(k) = \sum_{j:(i,j)\in E^a} x_{ij}^a(k)\mu_{ij}^{tx} + \sum_{j:(j,i)\in E^a} x_{ji}^a(k)\mu_i^{rx}$$

$$+ y_i(k)\phi_i^a \mu_i^{gn} - \left(b_i + \int_0^{\tau^a(k)} \rho_i^a(t)dt - \zeta_i \right)$$

and $\varepsilon(k)$ is the diminishing stepsize as in (31)-(32). Sensor i will send the updated Lagrangian multipliers $\lambda_i^a(k)$, $\nu_i^a(k)$ and $\xi_{ij}^a(k)$ to its direct neighbors to facilitate the computing of y_i and x_{ij}^a, while routing $\nu_i^a(k)$ and $\xi_{ij}^a(k)$ to the SenCar to calculate τ^a in the next iteration. Eq. (36) shows that if demand $y_i(k)\phi_i^a$ for sensor buffer at node i for caching the generated data exceeds the efficient storage space $\sum_{j:(i,j)\in E^a} x_{ij}^a(k) - \sum_{j:(j,i)\in E^a} x_{ji}^a(k)$, the flow conservation price λ_i^a will increase, which will in turn decrease the demand and increase the effective buffer. Meanwhile, (37) demonstrates that once the demand for energy consumption at sensor i for delivering, receiving and generating data is more than the maximum energy budget $\int_0^{\tau^a(k)} \rho_i^a(t)dt - \zeta_i$, the energy balance price ν_i^a will increase, which in turn will lead to the drop of demands for energy and the increase of available energy budget. We now provide the convergence analysis for lower-level subalgorithms of data control, joint scheduling and routing, and sojourn time allocation. For a given data split vector ϕ, denote $(\lambda^*, \nu^*, \xi^*)$ as the set of optimal solutions to the dual problem of problem (**OPT-2a**) $\min\limits_{\lambda,\nu,\xi\succeq 0} D(\phi,\lambda,\nu,\xi)$. Define $dist(p,S) = \min_{\overline{p}\in S} \|p - \overline{p}\|$ as the Euclidean distance of a point p to set S. Directly applying the convergence results for the subgradient method [25], we have the following theorem.

Theorem 1: If the stepsize $\varepsilon(k)$ satisfies the following condition

$$\lim_{k\to\infty} \varepsilon(k) = 0, \sum_{k=0}^{\infty} \varepsilon(k) = \infty, \tag{39}$$

then the Lagrangian multiplier iteration algorithm (36)-(38) converges, i.e.,

$$\lim_{k\to\infty} dist((\lambda(k), \nu(k), \xi(k)), (\lambda^*, \nu^*, \xi^*)) = 0. \tag{40}$$

Let $\mathbf{x}^*$, $\mathbf{y}^*$and τ^* be the sets of optimal values corresponding to λ^*, ν^* and ξ^*. By duality, immediately we have the following result.

Corollary 1: Under the same condition as in (39), the iterative subalgorithms of the data control (21), the joint scheduling and routing (25)-(27) and the sojourn time allocation (31)-(32) converge, i.e.,

$$\begin{aligned} &\lim_{k\to\infty} \|\mathbf{y}(k) - \mathbf{y}^*\| = 0, \\ &\lim_{k\to\infty} \|\mathbf{x}(k) - \mathbf{x}^*\| = 0, \\ &\lim_{k\to\infty} \|\tau(k) - \tau^*\| = 0. \end{aligned} \tag{41}$$

In our algorithm, for subgradient iteration k, we choose the diminishing stepsize as in (39) such that $0 < \varepsilon(k) < 1$ and $\varepsilon(k) = \alpha/(\beta k + \delta)$, where $\alpha > 0$, $\beta > 0$ and $\delta \geq 0$ are adjustable parameters that regulate the convergence speed. It was shown in [25] that regardless of the values of the initial Lagrangian multipliers, the diminishing stepsize can guarantee the convergence of the subalgorithms. Alternatively, in practical implementation, the stepsize can be chosen as a constant, which may induce that the subgradient method cannot converge to an optimal solution. By choosing a sufficiently small constant stepsize, however, the subgradient method can be made to converge within any given small neighborhood around the optimum.

B. Higher Level Optimization

The lower-level optimization subproblems of data control, joint scheduling and routing, and sojourn time allocation are solved under the assumption that each ϕ_i^a is fixed. At the higher level, we now explore how sensor i adjusts ϕ_i^a to achieve the optimum of WerMDG problem (**OPT-2)** by solving optimization problem (**OPT-2b**).

As aforementioned, $U(\phi)$ is the optimal objective value of problem (**OPT-2a)** over $\mathbf{x}$, $\mathbf{y}$ and τ. Then $U(\phi)$ can be expressed by

$$\begin{aligned} U(\phi) &= \min_{\lambda,\nu,\xi\succeq 0} D(\phi,\lambda^*, \nu^*, \xi^*) \\ &= \min_{\lambda,\nu,\xi\succeq 0} \max_{\mathbf{x},\mathbf{y},\tau} L(\phi, \mathbf{x}^*, \mathbf{y}^*, \tau^*, \lambda^*, \nu^*, \xi^*). \end{aligned} \tag{42}$$

Thus, we can characterize the marginal utility for ϕ_i^a by the partial derivative of $U(\phi)$ with respect to ϕ_i^a, $U'(\phi) = \frac{\partial U(\phi)}{\partial \phi_i^a} = -(\lambda_i^{a*} + \nu_i^{a*}\mu_i^{gn})y_i^*$, which reflects the changing rate of $U(\phi)$ with ϕ_i^a or the gain of data delivery from sensor i to anchor point a. Clearly, it is preferred that to maximize network utility $U(\phi)$, sensor i should always transfer some of its data destined to other anchor points to the one with higher gain until ϕ_i reaches equilibrium. If we let $\phi_i^* = \{\phi_i^{a*} | a \in \mathcal{A}\}$ be the optimal data split vector for sensor i, the optimal solution ϕ_i^{a*} to problem (**OPT-2b**) satisfies the following optimality condition, i.e.,

$$\phi_i^{a*} > 0 \Longrightarrow \frac{\partial U(\phi_i^*)}{\partial \phi_i^{a'}} \leq \frac{\partial U(\phi_i^*)}{\partial \phi_i^a}, \text{ for all } a' \in \mathcal{A}, \tag{43}$$

which implies that sensor i always sends more data to the anchor point that has the maximum marginal utility $U'(\phi)$.

For sensor i, assume that $\widetilde{a}$ denotes the anchor point with the maximum marginal utility, i.e., $\widetilde{a} = \arg\max_{a\in\mathcal{A}} \frac{\partial U(\phi)}{\partial \phi_i^a}$. Similar to [6], in the n-th iteration, sensor i can update ϕ_i^a according to

$$\phi_i^a(n+1) = \phi_i^a(n) + \delta_i^a(n), \tag{44}$$

$$\text{with } \delta_i^a(n) = \begin{cases} -\min\{\phi_i^a(n), \kappa(n)(\frac{\partial U(\phi)}{\partial \phi_i^{\widetilde{a}}}(n) - \frac{\partial U(\phi)}{\partial \phi_i^a}(n))\} \\ \qquad\qquad\qquad\qquad \text{if } a \neq \widetilde{a} \\ -\sum_{a\neq\widetilde{a}, a\in\mathcal{A}} \delta_i^a(n) \qquad \text{if } a = \widetilde{a} \end{cases}$$

where $\kappa(n)$ is a positive scalar stepsize. It is straightforward to verify that for sensor i

$$\sum_{a\in\mathcal{A}} \delta_i^a(n) = 0 \text{ and } \sum_{a\in\mathcal{A}} \delta_i^a(n) \frac{\partial U(\phi)}{\partial \phi_i^a} \geq 0. \tag{45}$$

We can see that $\sum_{a\in\mathcal{A}} \delta_i^a(n) \frac{\partial U(\phi)}{\partial \phi_i^a} = 0$ only if $\delta_i^a(n) = 0$, which requires that for all $a \in \mathcal{A}$

$$\phi_i^a(n) \left(\frac{\partial U(\phi)}{\partial \phi_i^{\widetilde{a}}}(n) - \frac{\partial U(\phi)}{\partial \phi_i^a}(n) \right) = 0. \tag{46}$$

This is exactly Wardrop equilibrium [29]. In other words, data split ratios per sensor node only settle when the gains of data delivered from sensor i to anchor point a have equalized (and thus are equal to the node marginal utility) and the remaining unused anchor points have lower gains.

We now study the convergence of such an updating algorithm on ϕ at the higher level by using a similar approach to that in [6]. For presentational convenience, we consider the continuous version of updating algorithm (44), which satisfies

$$\sum_{a\in\mathcal{A}} \dot{\phi}_i^a(n) = 0 \text{ and } \sum_{a\in\mathcal{A}} \frac{\partial U(\phi)}{\partial \phi_i^a} \dot{\phi}_i^a(n) \geq 0. \tag{47}$$

Similarly, we have $\sum_{a\in\mathcal{A}} \frac{\partial U(\phi)}{\partial \phi_i^a}\dot{\phi_i^a}(n) = 0$ only if $\dot{\phi_i^a}(n) = 0$, which holds only if (46) is satisfied. The updating algorithm (44) can be regarded as a specific discrete time implementation of (47).

Theorem 2: The updating algorithm (47) converges to the optimal solution of WerMDG problem (**OPT-2**).

Proof: From (16) and (42), we observe that $D(\phi,\lambda,\nu,\xi)$, as a function of λ,ν and ξ, includes the smooth terms and the non-smooth piece-wise linear terms. Hence, the differential of $U(\phi)$ can be rewritten as

$$\begin{aligned} dU(\phi) = &\left(\lim_{h\to 0^+} \frac{\partial D(\phi,\lambda^* + hd\lambda, \nu^*, \xi^*)}{\partial \lambda}\right) d\lambda \\ &+ \left(\lim_{h\to 0^+} \frac{\partial D(\phi,\lambda^*, \nu^* + hd\nu, \xi^*)}{\partial \nu}\right) d\nu \\ &+ \left(\lim_{h\to 0^+} \frac{\partial D(\phi,\lambda^*, \nu^*, \xi^* + hd\xi)}{\partial \xi}\right) d\xi \\ &+ \frac{\partial D(\phi,\lambda^*, \nu^*, \xi^*)}{\partial \phi} d\phi, \end{aligned} \tag{48}$$

where $(\lambda^*, \nu^*, \xi^*) = \arg \min\limits_{\lambda,\nu,\xi\succeq 0} D(\phi,\lambda,\nu,\xi)$. Since $(\lambda^*, \nu^*, \xi^*)$ minimizes $D(\phi,\lambda,\nu,\xi)$, for a given ϕ, we have

$$\lim_{h\to 0^+} \frac{\partial D(\phi,\lambda^* + hd\lambda, \nu^*, \xi^*)}{\partial \lambda}, \lim_{h\to 0^+} \frac{\partial D(\phi,\lambda^*, \nu^* + hd\nu, \xi^*)}{\partial \nu}$$

and $\frac{\partial D(\phi,\lambda^*,\nu^*,\xi^*+hd\xi)}{\partial \xi}$ cannot be in the decreasing direction. Accordingly, the first three terms in (48) are non-negative. Hence, we have

$$dU(\phi) \geq \frac{\partial D(\phi,\lambda^*, \nu^*, \xi^*)}{\partial \phi} d\phi, \tag{49}$$

That is,

$$\dot{U}(\phi) \geq \sum_{a\in\mathcal{A}} \sum_{i\in\mathcal{N}^a} \frac{\partial U(\phi)}{\partial \phi_i^a} \dot{\phi_i^a}(n) \geq 0, \tag{50}$$

which means that updating ϕ by (44) can always improve the overall network utility. In other words, for each sensor, when its positive marginal utility $U(\phi)$ keeps unchanged, i.e., cannot be improved, ϕ would reach equilibrium ϕ^*. Furthermore, updating algorithm (47) will converge to the optimal solution of problem (**OPT-2**). ■

Finally, we summarize the distributed algorithm for WerMDG problem in Table VI. In the inner (lower) loop, sensors search for optimal data rates and flow rates as well as optimal prices of flow conservation, energy balance and link capacity, while the SenCar determines optimal sojourn time at different anchors. In the outer (higher) loop, sensors adapt the data split vector based on the stabilized prices in the inner loop.

VI. Performance Evaluation

In this section, we conduct extensive simulations to evaluate WerMDG algorithm. Similar to many previous works, in the simulation, we adopt network utility function $U_i(\cdot) = w_i \log(\mathbf{y}_i + 1)$ to evaluate the network performance. The utility function represents the data uploaded from sensors and a sensor with a larger weight w_i would have more impact on the overall performance. As shown in the experiment in [13], the wireless energy transfer technique can deliver 60W power over a distance of 2m with 40% efficiency. We let the charging range be 2m and set the communication range of sensor nodes to be 10m.

A. Comparison of Single and Multi-Hop Data Collections

To justify our choice of using multi-hop data collections, we have conducted some simulations to compare data collection fairness and latency between single and multi-hop transmissions. Data collection fairness indicates whether data can be collected from all the sensor nodes. To quantify this value, we leverage the fairness index from [34],

$$F = \frac{(\sum_{i=1}^{n} x_i)^2}{n\sum_{i=1}^{n}(x_i)^2}. \tag{51}$$

where x_i is a normalized indicator which equals $1/|\mathcal{N}|$ if data is collected from node i, otherwise, it is 0, and $n = |\mathcal{N}|$ is the number of sensor nodes. The fairness index ranges from 0 (the worst case in which no data is collected) to 1 (the best case where data is collected from all the nodes). Fig. 3(a) shows the results with tour length threshold $L_{tsp} = 300, 400, 500$m, respectively. We can observe that fairness improves when we increase the data collection hop count. With single hop transmission ($l = 1$), the fairness is low. Once we increase the hop count to 2, fairness indices are improved significantly (e.g., fairness is increased by almost 100% if we use 2 hop transmission when $L_{tsp} = 400$m). Therefore, using multi-hop transmission improves the data collection fairness for nodes at different locations.

TABLE VI
Distributed algorithm for WerMDG problem

```
for each sensor $i \in \mathcal{N}$ do
  Initialize data split variable $\phi_i^a(0)$ for all $a \in \mathcal{A}$, $\sum_a \phi_i^a(0) = 1$;
  repeat
    Initialize Lagrangian multipliers $\lambda_i^a(0)$, $\nu_i^a(0)$ and $\xi_{ij}^a(0)$
    to non-negative values for all $j : (i,j) \in E^a$ and $a \in \mathcal{A}$;
    repeat: for all $j : (i,j) \in E^a$ and $a \in \mathcal{A}$
      Compute $y_i(k)$ by data control subalgorithm as shown in Table III;
      Compute $x_{ij}^a(k)$ by joint scheduling and routing subalgorithm
      as shown in Table IV;
      SenCar simultaneously computes $\tau^a$ by sojourn time allocation
      subalgorithm as shown in Table V;
      Update Lagrangian multipliers $\lambda_i^a(k+1)$, $\nu_i^a(k+1)$
      and $\xi_{ij}^a(k+1)$ by (36), (37) and ( 38) respectively;
      Send the updated Lagrangian multipliers to its direct neighbors
      and route $\nu_i^a(k+1)$ and $\xi_{ij}^a(k+1)$ to the SenCar;
    until $\{\lambda_i^a(k)\}$, $\{\nu_i^a(k)\}$ and $\xi_{ij}^a(k)$ converges to $\lambda_i^{a*}$, $\nu_i^{a*}$
    and $\xi_{ij}^{a*}$ respectively;
    Adjust data split variables $\phi_i^a(n+1)$ by (44);
  until $\{\phi_i^a(n)\}$ converges to $\phi_i^{a*}$;
end for
```

Furthermore, we show data collection latency in Fig. 3(b). We set $L_{tsp} = 300$m, change the number of nodes from 50 to 200 and evaluate average data collection latency for 6 intervals (with 60 min per interval). First, we can see that single-hop transmission results in the longest packet latency due to the very limited number of nodes visited by the SenCar per interval. Second, we observe that using 1 or 2 collection hops results in longer latency when we increase the number of nodes. In contrast, when the number of collection hops is 4, latency even decreases when we increase the number of nodes. This is because that when more nodes are present, connectivity in the network is improved with a larger collection hop count, which facilitates data transmissions and reduces data collection latency.

B. Convergence and Performance Analysis

First, we investigate the convergence property and analyze the performance of the proposed WerMDG algorithm. Fig. 4 shows the network topology for our evaluations. Specifically, we consider a rechargeable wireless sensor network with 40 sensor nodes uniformly randomly scattered over a $60 \times 60\ m^2$ field. The SenCar selects 5 anchor points (s^1 to s^5) for recharging sensors wirelessly and collecting data from the neighborhood. Since the data gathering algorithm is distributed and the energy replenishment of SenCar is independent of each other, WerMDG algorithm is also applicable

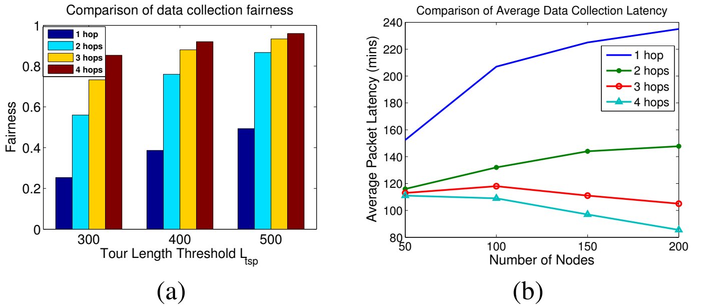

(a) (b)

Fig. 3. Comparison of single-hop and multi-hop transmission techniques. (a) Data collection fairness. (b) Average packet latency.

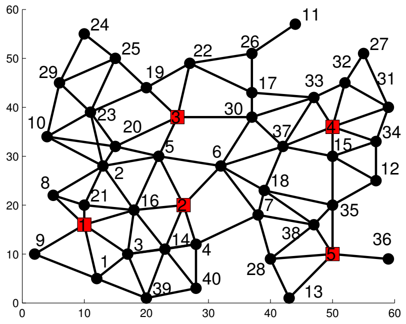

Fig. 4. Simulation Network Topology.

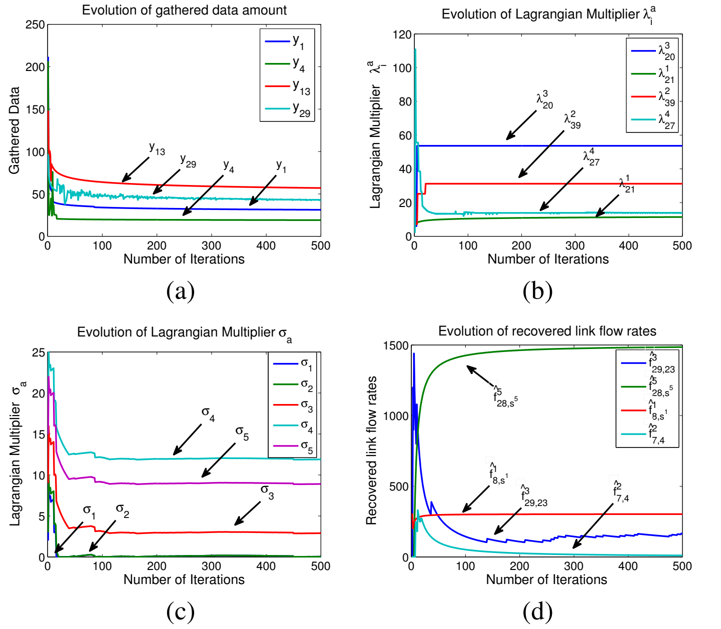

(a) (b)

(c) (d)

Fig. 5. Numerical results of convergence property of WERMDG algorithm (a) Evolution of the amount of data y_i vs. lower-level iterations; (b) Evolution of Lagrangian multiplier λ_i^a vs. lower-level iterations; (c) Evolution of Lagrangian multiplier σ_a for the SenCar vs. lower-level iterations; (d) Evolution of link flow rate $\widehat{f}_{ij}^a$ vs. lower-level iterations.

to large scale sensor networks. All the communication links carry the same capacity C_{ij}^c and the power consumption for transmitting a packet is proportional to the square of the distance between the sender and the receiver. Note that although the exact mathematical modeling for the recharge process of various commercial batteries or capacitors is difficult, statistically speaking, similar to the modeling of the discharge and charge process of capacitors or micro energy cells in [33] [30]. it is reasonable to model most of the recharge processes by a twice-differentiable, decreasing and strictly convex function, $\rho(t)^i = cB_i e^{-ct}$, where t is the time duration of recharge, and c is a constant related to the rate of recharging. All the parameters are summarized in Table VII.

Note that in order for variables to reach equilibrium in the higher-level optimization, the variables have to converge first in the lower-level optimization. For clarity, we show the convergence of some variables on selected sensors or links at the lower-level optimization, in which the diminishing stepsize is chosen. Fig. 5 shows the convergence of the algorithm in lower-level iterations. Fig. 5(a) depicts the evolution of total amount of data collected from sensors 1, 4, 13 and 29. We can see that the variables fluctuate in the first 30 iterations and reach equilibrium after 80 iterations. Similarly, Figs. 5(b) and (c) present the convergence of Lagrangian multipliers λ_i^a and σ_a, respectively. Fig. 5(d) shows the evolution of link flow rates on some selected links. We can see that link flow rates can converge to equilibrium in 350 iterations. In the meanwhile, the flow rate of a link with more hops converges more slowly than a link with fewer hops. For example, the flow rate of link (29, 23) with three hops to anchor point 3 (i.e., s^3) converges more slowly than that of link (8, s^1) with one hop to anchor point 1. The underlying reason behind such relationship is that for a link with a higher number of hops, its flow rate is influenced by remaining energy and buffer size of relay nodes, flow conservation cost of relay links and flow competition on these links. However, node degree has less impact on the convergence. For example, in Fig. 5(b), both nodes 39 and 27 are 2 hops away from their anchor points with degrees of 4 and 2, respectively. We notice that both Lagrangian multipliers can converge within 50 iterations.

TABLE VII
SIMULATION PARAMETERS

Parameter	Value	Parameter	Value
B	15mAh	$\mu_i^{(tx)}$	0.14 mW
$\mu_i^{(rx)}$	0.16 mW	$\mu_i^{(gn)}$	0.02 mW
w_i	500	$\pi_{ij}^{(k)}$	2 Kbits
c	2	T	30 min
inner stepsize $\varepsilon(k)$	$\frac{1}{(1+25k)}$	outer stepsize	0.005

After the variables have converged in the lower-level optimizations, we need to examine properties in higher-level optimization. For each sensor, we set the data split variables for different anchor points with equivalent values initially, i.e., $\phi_i^1 = \phi_i^2 = \phi_i^3 = \phi_i^4 = \phi_i^5 = 0.2$. We use a constant stepsize which equals 0.005 for the higher-level optimization. To reduce the number of lower-level iterations, we could assign the final values of Lagrangian multipliers in the higher-level optimization to the next run in lower-level optimization. Fig. 6 shows the evolution of total network utility and data split variables on sensor nodes 5, 11, 22 and 32. In Fig. 6(a), the total network utility surges greatly in the first 10 iterations and then fluctuates slightly within 5% of the optimal value. It is justifiable since the convergence of network utility on different sensors is not synchronized, while it also differs for different anchor points. In Fig. 6(b), the evolution of data split variables is plotted for sensors nodes 5, 11, 22 and 32. At the optimal state, sensor 5 and 11 will send nearly 50% of its data to anchor point 3, sensor 22 will send 40% of its data to anchor point 2 and sensor 32 will send all of its data to anchor point 4, which shows that a sensor always prefers to transfer more data destined to the anchor point with higher gain of data delivery. The reason is that the data split ratio for different anchor points depends on the gains of links from a sensor to anchor points and the prices of both flow conservation and energy balance at sensor nodes on these links. From Figs. 6 (a) and (b), we can see that the update of data split variables clearly helps improve the convergence of

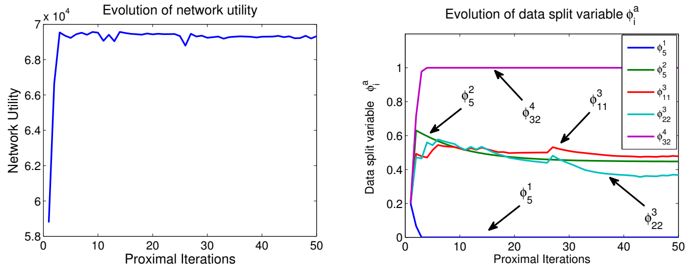

(a) (b)

Fig. 6. Numerical results of convergence property of WerMDG algorithm (a) Evolution of total network utility vs. higher-level iterations; (b) Evolution of data split variable ϕ_i^a vs. higher-level iterations.

TABLE VIII
OPTIMAL SOJOURN TIME ALLOCATION

Anchor Points	1	2	3	4	5
Time (minutes)	0.45	0.66	1.96	2.99	2.38

network utility.

In addition, we provide the optimal sojourn time for SenCar at each anchor point in Table VIII. It is observed from the table that the sojourn time for different anchor points can vary from each other. For example, for the topology shown in Fig. 4, the sojourn time SenCar spent at anchor points 1, 2 and 3 is much less than the time SenCar spent at anchor points 4 and 5, which indicates that sojourn time is a variable depending on the prices of energy balance and link capacity and the rate of the energy replenishment at each anchor point.

C. Impact of Utility Weight on Performance

Next, we examine the impact on performance by adjusting the utility weight at selected sensors. The purpose to assign different weights to sensors in various locations is to control the order of preference for the SenCar when collects data from them. Here, we linearly increase w_i on sensors $\{1, 2, 3, 4, 8, 9\}$ from 500 to 3000 while keeping w_i at 500 for all other sensors. Fig. 7(a) and (b) show the impact of utility weight on the amount of data gathered from sensors and anchor points, respectively. In Fig. 7(a), compared to sensor node 16, whose utility weight is kept unchanged, the amount of data collected for sensor nodes 1, 3 and 8 increases with utility weight. Furthermore, notice that the amount of data collected even declines with the increase of utility weight from sensor node 16 around anchor point 1. It indicates that the SenCar is able to collect more data from designated sensors by assigning a larger utility weight to them and sensors with lower utility weight might have to give up some data uploading opportunities to sensors with higher utility weight. Fig. 7(b) presents the amount of data collected at anchor points 1, 2 and 3. Similarly, the amount of data collected at anchor points closed to sensor nodes 1, 2, 3, 4, 8 and 9 increases with a higher utility weight.

D. Impact of Recharging Rate on Performance

In this subsection, we adjust the rate of recharging to see the effect on network performance. Recall that we used recharging function $\rho(t)^i = aB_ie^{-at}$ in our simulation to mimic the recharging process of capacitors. Here, a determines the rate of recharging. A larger a results in a faster battery refill to its full capacity B_i. In practice, the recharging rate of a capacitor depends on the resistance and capacitance in the circuitry. Fig. 8(a) shows the total network utility when a increases from 1 to 2. It is observed that the total network utility in one data gathering tour slightly decreases with recharging rate a . Fig. 8(b) presents the SenCar's sojourn time at each anchor point with different recharging rates a. We can see that the trend of network utility in one data gathering tour and sojourn time decrease with the increase of the recharging rate. This is because a higher recharging rate will result in the sensor battery to be refilled in shorter time and once the battery has been refilled at an anchor point and data collection is completed, the SenCar can move to the next anchor point. Thus, the SenCar is able to make more recharge tours during a fixed interval when the sojourn time at each sensor node has been shortened. Therefore, exploiting a higher recharge rate is beneficial to the performance of the network in terms of utility, lifetime and scalability. Once the recharge duration of each sensor can be further reduced based on future battery technologies [31], it can certainly guarantee the perpetual operations of the network.

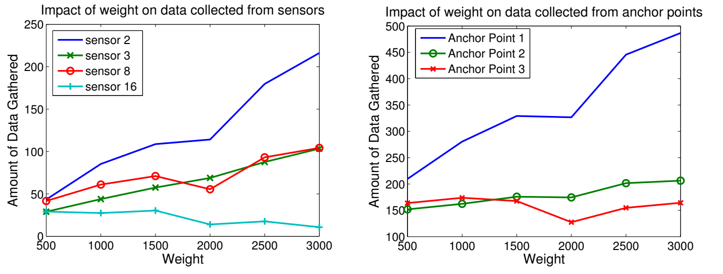

(a) (b)

Fig. 7. Impact of utility weight on network performance (a) impact of utility weight on amount of data gathered from sensors (b) impact of utility weight on amount of data gathered at anchor points.

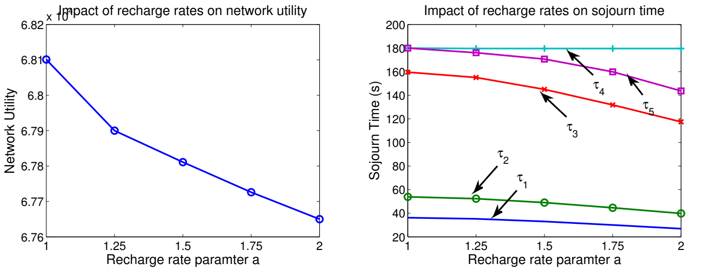

(a) (b)

Fig. 8. Impact of recharging rate (a) impact of recharging rate on total network utility (b) impact of recharging rate on SenCar sojourn time.

E. Network-Wide Performance

To justify that the WerMDG algorithm can work well in a realistic network environment, we also implement it in the NS-2 simulator [32]. NS-2 is a discrete event-driven simulator targeted at networking research, and can simulate the dynamics of almost all network protocols. In this simulation, we implement the data control subalgorithm at the transport layer and the joint scheduling and routing subalgorithm at the network layer based on Ad hoc On-Demand Distance Vector Routing (AODV), which is used as the routing protocol. Unless otherwise stated, the default parameter settings are as follow: the two-ray ground reflection model is used as the radio propagation model, IEEE 802.11 DCF (Distributed Coordination Function) as the MAC protocol, Drop Tail as the interface queue type and Omniantenna as the antenna model. An interface queue at the MAC layer could hold 50 packets before they are sent out to the physical link. Link breakage is detected from MAC layer feedbacks. A routing buffer at the network layer could store up to 64 data packets. This buffer keeps data packets waiting for a route, such as packets for which route discovery has

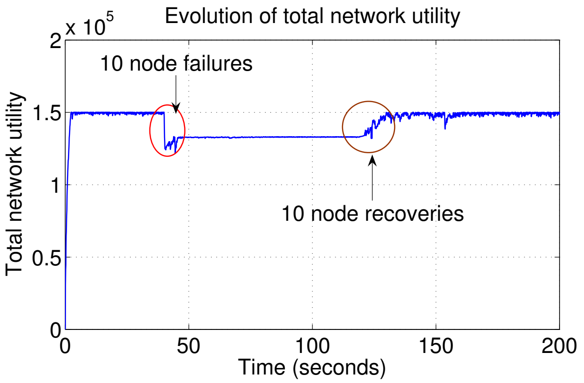

Fig. 9. Evolution of total network utility in case of 10 node failures and 10 node recoveries.

started but no reply arrived yet. We assume that all results are averaged over 100 random simulations and each simulation lasts 200 seconds.

In this simulation, 100 sensor nodes are randomly scattered in a 1,000m by 1,000m square area and 15 anchor points are selected. All the parameter settings are the same as those in Table VII. A mobile node is regarded as the SenCar performing both data gathering and wireless recharging. We first verify the feasibility of the WerMDG algorithm in a realistic network environment and its fault-tolerate ability in case of sudden node failures. We assume that at the 40th second, 10 nodes become invalid and withdraw from sensing due to that they are attacked or their energy is drained; at the 120th second, 10 nodes renew to come into the network and recover sensing due to that they are released by attackers or get recharged wirelessly. Fig. 9 illustrates the evolution of total network utility of all sensors in case of node failures. We can draw the underlying observations. First, the proposed WerMDG algorithm can be implemented and get converged in NS-2 environment. Second, at the 40th second, total network utility decreases evidently and then gradually keep stable due to node sudden failure. The reason behind the observation is that the sudden failures of 10 nodes break the previous scheduling and routing balance, and force the sources to discover new data forwarding routes, which in turn leads to the increase of flow conservation prices and the decreases of total network utility. Third, at the 120th second, as 10 nodes re-join the network, total network utility get also recovered to the level before failures. These observations implies that the WerMDG algorithm can work well in real network settings and environment and can converge fast even if it suffers from sudden node failures.

We now further explore the performance comparison between the WerMDG algorithm and other mobile data gathering strategies such as Packet Transmission Scheduling (PTS) Algorithm in [12] and J-MERDG in [8] in terms of total network utility and relative network lifetime. Here, $x\%$ *network lifetime* is defined as the network lifetime when $(100-x)\%$ sensors either run of battery or cannot send data to the data sink due to the failure of relaying nodes. Fig. 10 shows comparison of total network utility and relative network lifetime among WerMDG, PTS and J-MERDG. It can be seen from Fig. 10(a) that as the bound of total sojourn time T increases, the total network utility of all three data gathering algorithms increases as well. Compared to PTS and J-MERDG, however, the WerMDG algorithm has the larger network utility for a given T. The reason is that the long sojourn time can lead to the more data the SenCar collects, which induces the increase of total network utility. It can be observed from Fig. 10(b) that with the increase of total sojourn time, the relative network lifetime decreases. Compared to PTS and J-MERDG, however, the network lifetime of the WerMDG algorithm can be prolonged significantly for a given T. This is justifiable since, although the PTS strategy takes into account of the tradeoff between the energy consumption and the probability of successful packet arrival at the sink, it does not consider energy replenishment for sensor nodes. As a result, the longer the sojourn time of SenCar, the more the energy consumption of sensors. On the other hand, compared to J-MERDG, the WerMDG algorithm considers the comprehensive sources of energy consumption and the time-varying nature of energy recharging.

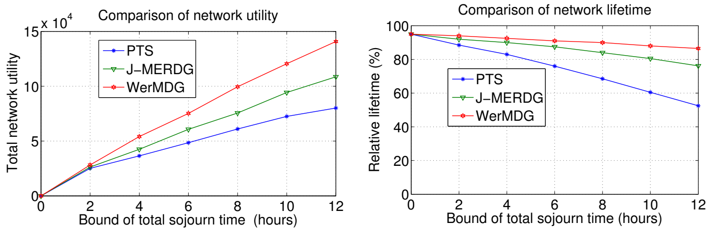

(a) (b)

Fig. 10. (a) Comparison of total network utility over bound of total sojourn time (b) Comparison of relative network lifetime over bound of total sojourn time.

VII. Conclusions

In this paper, we have studied the problem of joint wireless energy replenishment and mobile data gathering (WerMDG) for rechargeable sensor networks. In particular, a multi-functional SenCar is deployed in the sensing field to charge the visited sensors via wireless energy transfer and simultaneously collect data from nearby sensors via multi-hop transmissions. We first present an anchor point selection algorithm to determine the sensors that should get recharged in priority and the sequence of the anchor points that the SenCar visits. We then formulate the WerMDG problem into a network utility maximization problem by taking into account the overall energy consumption and the time-varying recharging rate. Furthermore, we propose a distributed cross-layer WerMDG algorithm, through which each sensor adaptively tunes its optimal data rates and routing paths based on the current energy replenishment status while the SenCar dynamically adjusts its optimal sojourn time at each anchor point such that the entire network utility can be maximized. Last, we provide extensive numerical results to demonstrate that the proposed WerMDG algorithm converges, and verify the impact of utility weight and recharging rate on network performance in terms of the amount of data gathered, network utility, link flow rate and sojourn time allocation. The simulation results also show that the WerMDG algorithm can work well in real network settings and environment and can converge fast even if it suffers from sudden node failures.

Finally, we would like to point out that there are some interesting issues that may be studied in our future work. First, a hybrid scheme combining static data transmission to the sink with mobile data gathering may be considered for high density and connected sensor networks since it may reduce the traveling time of the SenCar thus data collection latency. It poses some new challenges such as determining whether it is beneficial for a sensor node to forward data to the sink or to the SenCar since the anchor points may change from time to time. Second, for a high density network, where channel contentions and packet collisions from the MAC layer have an impact on the optimal strategies, a cross-layer approach considering both routing and MAC layer also needs to be studied in future.

VIII. Acknowledgments

The work in this paper was supported in part by the grants from the National Natural Science Foundation of China (61170248,61373179,61373178), New Century Excellent Talents in University (No. NCET-10-0877), Natural Science Foundation of Chongqing (CSTC, cstcjjA40003), Science and Technology Leading Talent Promotion Project of Chongqing (cstc2013kjrc-ljrccj40001), Fundamental Research Funds for the Central Universities (XDJK2013A018), and US National Science Foundation under grant number ECCS-1307576 and US Army Research Office under grant number W911NF-09-1-0154.

References

[1] K.-W. Fan, Z. Zheng, and P. Sinha, "Steady and fair rate allocation for rechargeable sensors in perpetual sensor networks," *ACM SenSys* 2008, pp. 239-252.

[2] M. Ma and Y. Yang, "SenCar: An energy efficient data gathering mechanism for large scale multihop sensor networks," *IEEE Trans. Parallel and Distributed Systems*, vol. 18, no. 10, pp. 1476-1488, 2007.

[3] R.-S. Liu, K.-W. Fan, Z. Zheng and P. Sinha, "Perpetual and fair data collection for environmental energy harvesting sensor networks," *IEEE/ACM Trans. Networking*, vol. 19, no. 4, pp. 947-960, Aug. 2011.

[4] M. Ma, Y. Yang and M. Zhao, "Tour planning for mobile data gathering mechanisms in wireless sensor networks," *IEEE Trans. Vehicular Technology,* vol. 62, no. 4, pp. 1472-1483, May 2013.

[5] S. Chen, P. Sinha, N. Shroff and C. Joo, "Finite-horizon energy allocation and routing scheme in rechargeable sensor networks," *IEEE INFOCOM, 2011*, April 2011, pp. 2273-2281.

[6] M. Zhao and Y. Yang, "Optimization based distributed algorithms for mobile data gathering in wireless sensor networks," *IEEE Trans. Mobile Computing*, vol. 11, no. 10, pp. 1464-1477, Oct. 2012.

[7] R.-S. Liu, P. Sinha and C. Koksal, "Joint energy management and resource allocation in rechargeable sensor networks," *IEEE INFOCOM, 2010*, March 2010.

[8] M. Zhao, J. Li, and Y. Yang, "Joint mobile energy replenishment and data gathering in wireless rechargeable sensor networks," *IEEE ITC*, 2011, pp. 238-245.

[9] M. Zhao, M. Ma and Y. Yang, "Efficient data gathering with mobile collectors and space-division multiple access technique in wireless sensor networks," *IEEE Trans. Computers*, vol. 60, no. 3, pp. 400-417, 2011.

[10] M. Zhao and Y. Yang, "Bounded relay hop mobile data gathering in wireless sensor networks," *IEEE Trans. Computers*, vol. 61, no. 2, pp. 265-271, Feb. 2012.

[11] J. Papandriopoulos, S. Dey, and J. Evans, "Optimal and distributed protocols for cross-layer design of physical and transport layers in MANETs," *IEEE/ACM Trans. Networking*, vol.16, no. 6, pp. 1392-1405, Dec. 2008.

[12] A. Sharifkhani and N. C. Beaulieu, "A mobile-sink-based packet transmission scheduling algorithm for dense wireless sensor networks," *IEEE Trans. Vehicular Technology*, vol. 58, no. 8, pp. 2509-2518, 2009.

[13] A. Kurs, A. Karalis, R. Moffatt, J. D. Joannopoulos, P. Fisher and M. Soljacic, "Wireless power transfer via strongly coupled magnetic resonances," *Science*, vol. 347, no. 5834, pp. 83-86, July 2007.

[14] J. Makare, "Wireless resonant energy link (wrel) demo," August 2011. [Online]. Available: *http://brightcove.vo.llnwd.net/pd16/media/740838651001/740838651001_1127592260001_R-ID-David-Meyer-V1.mp4*

[15] M. Erol-Kantarci and H. T. Mouftah, "Suresense: sustainable wireless rechargeable sensor networks for the smart grid," *IEEE Wireless Communications*, vol. 19, no. 3, pp. 30-36, June 2012.

[16] T.-C. Chiu, Y.-Y. Shih., A.-C. Pang, J.-Y. Jeng and P.-C. Hsiu, "Mobility-aware charger deployment for wireless rechargeable sensor networks," *14th Asia-Pacific APNOMS*, 2012, pp. 1-7.

[17] S. He, J. Chen,F. Jiang, D. K.Y. Yau, G. Xing and Y. Sun, "Energy provisioning in wireless rechargeable sensor networks," *IEEE Trans. Mobile Computing*, vol. 12, no. 10, pp. 1931-1942, Oct. 2013.

[18] Y. Shi, L. Xie, Y. Hou, and H. Sherali, "On renewable sensor networks with wireless energy transfer," *IEEE INFOCOM*, 2011, pp. 1350-1358.

[19] S. Guo, C. Wang and Y. Yang, "Mobile data gathering with wireless energy replenishment in rechargeable sensor networks," *IEEE INFOCOM*, pp. 1932-1940, 2013.

[20] B. Zhang, R. Simon, and H. Aydin, "Maximum utility rate allocation for energy harvesting wireless sensor networks," in *Proc. of the 14th ACM MSWiM*. 2011, pp.7-16.

[21] J.-W. Lee, R. R. Mazumdar, and N. B. Shroff, "Joint opportunistic power scheduling and end-to-end rate control for wireless ad hoc networks," *IEEE Trans. Vehicular Technology*, vol. 56, no. 2, pp. 801-809, Mar. 2007.

[22] K. Hedayati, I. Rubin, and A. Behzad, "Integrated power controlled rate adaptation and medium access control in wireless mesh networks," *IEEE Trans. Wireless Comm.*, vol. 9, no. 7, pp. 2362-2370, Jul. 2010.

[23] W. R. Heinzelman, A. Chandrakasan and H. Balakrishnan, "Energy-efficient communication protocol for wireless microsensor networks," *IEEE HICSS*, 2000.

[24] T.H. Cormen, C. E. Leiserson, R. L. Rivest and C. Stein, *Introduction to Algorithms*, MIT Press, 2001.

[25] S. Boyd and L. Vandenbergh, *Convex Optimization*. Cambridge University Press, 2004.

[26] M. Chiang, S. Low, A. Calderbank and J. Doyle, "Layering as optimization decomposition: A mathematical theory of network architectures," *Proc. of the IEEE*, vol. 95, no. 1, pp. 255-312, Jan. 2007.

[27] L. Chen, S. H. Low, M. Chiang, and J. C. Doyle, "Cross-layer congestion control, routing and scheduling design in ad hoc wireless networks," *IEEE INFOCOM*, April 2006, pp. 1-13.

[28] G. Hanif D. Sherali, "Recovery of primal solutions when using subgradient optimization methods to solve lagrangian duals of linear programs," *Operations Research Letters*, vol. 19, no. 3, pp. 105-113, 1996.

[29] J. G. Wardrop, "Some theoretical aspects of road traffic research," *Proc. of the Institution of Civil Engineers, Part II*, vol. 1, 1952, pp. 325-378.

[30] D. Irwin and R. Nelms, *Basic Engineering Circuit Analysis*, Wiley, 2010.

[31] B. Kang and G. Ceder, "Battery materials for ultrafast charging and discharging,"*Nature*, vol. 458, pp. 190-193, 2009.

[32] NS-2, Network Simulator, *http://www.isi.edu/nsnam/ns/*, 2012.

[33] Website: "http://hyperphysics.phy-astr.gsu.edu/hbase/electric/capdis.html."

[34] R. Jain, D. M. Chiu, W. Hawe, "A quantitative measure of fairness and discrimination for resource allocation in shared computer systems," *DEC Research Report TR-301*.

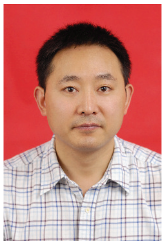

Songtao Guo received his B.S., M.S. and Ph.D. degrees in Computer Software and Theory from Chongqing University, Chongqing, China, in 1999, 2003 and 2008, respectively. He was a professor from 2011 to 2012 at Chongqing University. At present, he is a full professor at Southwest University, China. He was a senior research associate at the City University of Hong Kong from 2010 to 2011, and a visiting scholar at Stony Brook University, New York, USA, from May 2011 to May 2012. His research interests include wireless sensor networks, wireless ad hoc networks and parallel and distributed computing. He has published more than 30 scientific papers in leading refereed journals and conferences. He has received many research grants as a Principal Investigator from the National Science Foundation of China and Chongqing and the Postdoctoral Science Foundation of China.

Cong Wang received the BEng degree of Information Engineering from the Chinese University of Hong Kong in 2008, and MS degree in Electrical Engineering from Columbia University, New York, in 2009. He is currently working towards the PhD degree at the Department of Electrical and Computer Engineering, Stony Brook University, New York. His research interests include wireless sensor networks, performance evaluation of network protocols and algorithms.

Yuanyuan Yang received the BEng and MS degrees in computer science and engineering from Tsinghua University, Beijing, China, and the MSE and PhD degrees in computer science from Johns Hopkins University, Baltimore, Maryland. She is a professor of computer engineering and computer science at Stony Brook University, New York, and the director of Communications and Devices Division at New York State Center of Excellence in Wireless and Information Technology (CEWIT). Her research interests include wireless networks, data center networks, optical networks and high-speed networks. She has published 280 papers in major journals and refereed conference proceedings and holds seven US patents in these areas. She is currently the Associate Editor-in-Chief for the IEEE Transactions on Computers and an Associate Editor for the Journal of Parallel and Distributed Computing. She has served as an Associate Editor for the IEEE Transactions on Computers and IEEE Transactions on Parallel and Distributed Systems. She has served as a general chair, program chair, or vice chair for several major conferences and a program committee member for numerous conferences. She is an IEEE Fellow.